

RESEARCH ARTICLE

Rescue of ATXN3 neuronal toxicity in *Caenorhabditis elegans* by chemical modification of endoplasmic reticulum stress

Yasmin Fardghassemi^{1,2,*}, Arnaud Tauffenberger^{1,3,*}, Sarah Gosselin^{1,4} and J. Alex Parker^{1,2,3,4,†}

ABSTRACT

Polyglutamine expansion diseases are a group of hereditary neurodegenerative disorders that develop when a CAG repeat in the causative genes is unstably expanded above a certain threshold. The expansion of trinucleotide CAG repeats causes hereditary adult-onset neurodegenerative disorders, such as Huntington's disease, dentatorubral–pallidoluysian atrophy, spinobulbar muscular atrophy and multiple forms of spinocerebellar ataxia (SCA). The most common dominantly inherited SCA is the type 3 (SCA3), also known as Machado–Joseph disease (MJD), which is an autosomal dominant, progressive neurological disorder. The gene causatively associated with MJD is *ATXN3*. Recent studies have shown that this gene modulates endoplasmic reticulum (ER) stress. We generated transgenic *Caenorhabditis elegans* strains expressing human *ATXN3* genes in motoneurons, and animals expressing mutant *ATXN3*–CAG89 alleles showed decreased lifespan, impaired movement, and rates of neurodegeneration greater than wild-type *ATXN3*–CAG10 controls. We tested three neuroprotective compounds (Methylene Blue, guanabenz and salubrinal) believed to modulate ER stress and observed that these molecules rescued *ATXN3*–CAG89 phenotypes. Furthermore, these compounds required specific branches of the ER unfolded protein response (UPR^{ER}), reduced global ER and oxidative stress, and polyglutamine aggregation. We introduce new *C. elegans* models for MJD based on the expression of full-length *ATXN3* in a limited number of neurons. Using these models, we discovered that chemical modulation of the UPR^{ER} reduced neurodegeneration and warrants investigation in mammalian models of MJD.

KEY WORDS: Ataxin 3, *Caenorhabditis elegans*, Endoplasmic reticulum stress, Guanabenz, Polyglutamine

INTRODUCTION

Polyglutamine (poly-Q) expansion diseases are a class of dominantly inherited neurodegenerative disorders that develop when there is an abnormal expansion, and subsequent translation, of trinucleotide CAG repeats (Gatchel and Zoghbi, 2005; Matos et al., 2011; Shao and Diamond, 2007; Xu et al., 2015). These diseases are characterized by

a selective loss of neurons along with physical and psychological complications (Matos et al., 2011). Indeed, the abnormal expansion of polyglutamine induces numerous pathological changes in patients, including modifications of the proteome leading to functional alterations, generation of toxic poly-Q protein species, protein aggregation, transcriptional dysregulation, proteotoxic stress and mitochondrial dysfunction (Shao and Diamond, 2007). However, the exact mechanism of disease pathogenesis is still not well understood. The poly-Q expansion diseases include several neurodegenerative disorders, such as Huntington's disease, dentatorubral–pallidoluysian atrophy, spinobulbar muscular atrophy and six forms of spinocerebellar ataxia (SCA) (Matos et al., 2011; Teixeira-Castro et al., 2015). SCAs are considered to be rare disorders, with a prevalence ranging from 0.3 to 2.0 per 100,000 (van de Warrenburg et al., 2002). SCA3 (spinocerebellar ataxia type 3), also known as Machado–Joseph disease (MJD), is considered to be the most common form of SCA worldwide (Schöls et al., 2004).

MJD is an autosomal dominant progressive neurological disorder characterized principally by ataxia, spasticity, peripheral neuropathy and ocular movement abnormalities (França et al., 2008). This disease is accompanied by neurodegeneration in selective regions, mainly in the cerebellum, basal ganglia, brainstem and spinal cord (Teixeira-Castro et al., 2011, 2015; Matos et al., 2011). Regarding brain function, it has been shown that metabolism is decreased in several regions of the nervous system, such as the cerebellum, brainstem and cerebral cortex, along with negative perturbations in both dopaminergic and cholinergic neurotransmission (Soon et al., 1997; Wüllner et al., 2005; Yen et al., 2000; Riess et al., 2008; Rub et al., 2008). MJD, constituting the most prevalent subtype of SCA, is more frequently observed among people of Portuguese/Azorean ancestry, with the highest prevalence in the Azorean island of Flores (1/239; Bettencourt et al., 2008). The gene causatively associated with MJD is *ATXN3* (ataxin 3) and is located on chromosome 14 (14q24.3–14q32.45; Kawaguchi et al., 1994; Takiyama et al., 1994). This gene encodes a poly-Q-containing protein named ataxin 3 (Kawaguchi et al., 1994).

Ataxin 3 has 339 amino acid residues, with an estimated molecular weight of 42 kDa for normal individuals (Kawaguchi et al., 1994). Healthy individuals have between 10–51 CAG repeats, which is expanded to 55–87 repeats in the disease state (Maciel et al., 2001; Cummings and Zoghbi, 2000). Ataxin 3 has several functional domains, including the N-terminus of the catalytic Josephin domain that presents a globular and a very conserved structure, followed by two ubiquitin interacting motifs (UIM) that are also considered as conserved regions, the poly-Q domain and finally, depending on the protein isoform, a third atypical UIM in the C-terminus tail (Goto et al., 1997; Li et al., 2015).

To aid the study of MJD, we turned to the model organism *Caenorhabditis elegans*. This nematode is 1 mm long, easy to maintain in laboratory settings, highly amenable to genetic manipulation, and is especially well suited for neuroscience

¹Centre de recherche du Centre hospitalier de l'Université de Montréal (CRCHUM) Montréal, Québec H2X 0A9, Canada. ²Département de biochimie et médecine moléculaire, Université de Montréal, Montréal, Québec H3T 1J4, Canada.

³Département de pathologie et biologie cellulaire, Université de Montréal, Montréal, Québec H3T 1J4, Canada. ⁴Département de neurosciences, Université de Montréal, Montréal, Québec H3T 1J4, Canada.

*These authors contributed equally to this work

†Author for correspondence (ja.parker@umontreal.ca)

DOI: J.A.P., 0000-0002-3333-2445

This is an Open Access article distributed under the terms of the Creative Commons Attribution License (<http://creativecommons.org/licenses/by/3.0>), which permits unrestricted use, distribution and reproduction in any medium provided that the original work is properly attributed.

research because of its comprehensively detailed neuronal lineage and interconnectivity of synapses that resembles aspects of the vertebrate nervous system (Stiernagle, 2006). Additionally, the *C. elegans* genome contains an orthologue of *ATXN3*, named *atx-3*. The *C. elegans* orthologue of human ataxin 3 is localized in both the nucleus and the cytoplasm, with higher levels observed in the cytoplasm. It has been shown that loss of *atx-3* activity results in changes in the expression of genes involved in several different pathways: the ubiquitin–proteasome pathway, signal transduction and cell structure and motility (Rodrigues et al., 2007; Kawaguchi et al., 1994). Ataxin 3 has been identified as participating in the endoplasmic reticulum network (Matos et al., 2011; Echtermeyer et al., 2011; Reina et al., 2010). We previously showed that several compounds, including Methylene Blue, salubrinal and guanabenz, target the endoplasmic reticulum (ER) stress response and protect against proteotoxicity in simple models of amyotrophic lateral sclerosis (ALS; Vaccaro et al., 2013, 2012a) and have beneficial effects in models of the neurological disorder hereditary spastic paraplegia (Julien et al., 2016). In this study, using our transgenic *C. elegans* *ATXN3* models, we explored whether small molecules that regulate ER stress response activity were able to rescue locomotor phenotypes, neuronal loss and the increased oxidative and ER stress observed in mutant transgenic animals as an early effort for MJD therapy development.

RESULTS

Expression of full-length human *ATXN3* in *C. elegans*

Using Mos1-mediated single copy insertion (MoSci) transposon-mediated single copy insertion into the genome (Frokjaer-Jensen et al., 2014), we created strains to model MJD by expressing full-length, human *ATXN3* in *C. elegans*. It has been shown previously that expressing ataxin 3 with 89 CAG repeats (CAG89) results in neurodegeneration, and in protein misfolding phenotypes in cell culture and *Drosophila* models (Stochmanski et al., 2012). Based on our previous neurodegeneration models (ALS models), we expressed human *ATXN3*, either wild-type *ATXN3-CAG10* (Fig. 1A) or mutant *ATXN3-CAG89* (Fig. 1B), in the worm's 26 GABAergic motoneurons using the promoter for the gene *unc-47*, which encodes a vesicular GABA transporter (Vaccaro et al., 2012a). In our experience, the *unc-47* modelling approach produces animals with strong phenotypes resulting from the expression of disease-associated proteins in a small number of neurons. Thus, in the context of chemical suppressor screens, relatively few neurons need to be exposed to small molecules to detect reversion of phenotypes.

We confirmed the expression of full-length human *ATXN3* in transgenic *C. elegans* strains by western blotting with a human specific anti-*ATXN3* antibody. A band corresponding to wild-type *ATXN3-CAG10* and a larger band for the MJD-associated mutant *ATXN3-CAG89* were detected by western blotting of worm protein extracts. However, the anti-*ATXN3* also detected a band in non-transgenic wild-type N2 animals (Fig. 1C). *atx-3* encodes a deubiquitylating enzyme that is the highly conserved *C. elegans* orthologue of human *ATXN3* (Kawaguchi et al., 1994; Echtermeyer et al., 2011), thus it can be detected by western blotting with a human specific *ATXN3* antibody. To confirm this, we conducted western blotting experiments using the anti-*ATXN3* antibody and protein extracts from *atx-3* null mutants. *atx-3(tm1689)* is a loss-of-function mutation consisting of a 660 bp deletion along with a 6 bp insertion (*C. elegans* Deletion Mutant Consortium, 2012; Rodrigues et al., 2007), and no signal was observed. These data suggest that the anti-*ATXN3* antibody recognizes *C. elegans* ATX-3 in N2 wild-type worms and partly obscures the signal for *ATXN3-CAG10*

transgenics, but a specific, higher molecular weight signal is visible in extracts from *ATXN3-CAG89* animals (Fig. 1C). Finally, we confirmed the specificity of the anti-*ATXN3* antibody by western blotting using protein extracts from cells originating from healthy controls or MJD patients (Fig. 1D).

Decreased lifespan and impaired neuronal phenotypes in mutant *ATXN3* transgenics

We wondered whether the expression of non-native proteins led to decreased health in the transgenic strains. Initially, we investigated whether lifespan was altered in our *ATXN3* transgenics. Using age-synchronized animals we observed that both *ATXN3-CAG10* and *ATXN3-CAG89* transgenics showed significantly decreased lifespan compared with non-transgenic wild-type N2 worms (Fig. 2A). These data demonstrate that increased expression of *ATXN3* transgenes has negative consequences on lifespan, but the mutant *ATXN3-CAG89* transgene had a more severe phenotype compared with *ATXN3-CAG10* controls.

Decreased lifespan can indicate poor health of the animals, and one sign of ageing in *C. elegans* is decreased motility that can be quantified using assays for progressive, age-dependent paralysis (Collins et al., 2008; Herndon et al., 2002). We observed that the age-synchronized *ATXN3-CAG89* transgenics displayed progressive motor defects compared with wild-type *ATXN3-CAG10* transgenics. Starting during adulthood, *ATXN3-CAG89* transgenics displayed uncoordinated motility phenotypes, progressing to paralysis over a period of 12 days, and occurred at a higher rate compared with *ATXN3-CAG10* controls (Fig. 2B).

The nematode *C. elegans* body wall muscle cells receive excitatory (acetylcholine) and inhibitory (GABA) inputs to coordinate muscle contraction and relaxation and to facilitate movement (McIntire et al., 1993). Activity of the neuromuscular junction can be measured indirectly with the acetylcholinesterase inhibitor aldicarb (Mahoney et al., 2006). It has been shown that treating worms with the known compound, aldicarb, results in accumulation of acetylcholine at neuromuscular junctions, leading to a number of different phenotypes: hyperactive cholinergic synapses, muscle hypercontraction and acute paralysis (Mahoney et al., 2006). Mutant strains having a defect in synaptic vesicle release demonstrate resistance for aldicarb. Resistance or hypersensitivity to aldicarb-induced paralysis has been used to identify genes that regulate acetylcholine secretion or inhibitory GABA signalling in different studies, including ours for ALS models (Loria et al., 2004; Vaccaro et al., 2012b). To investigate whether our transgenic *ATXN3* strains had abnormal activity at the neuromuscular junction, we exposed them and two control strains, *unc-64(e246)* (resistant to aldicarb, encodes syntaxin) and *unc-47(e307)* (hypersensitive to aldicarb), to aldicarb. Transgenic *ATXN3-CAG89* strains and *unc-47(e307)* mutants were hypersensitive to aldicarb-induced paralysis compared with *ATXN3-CAG10* transgenics, wild-type N2 worms, and *unc-64(e246)* mutants at days 1, 5 and 9 of adulthood (Fig. 2C). *ATXN3-CAG10* transgenics did show a hypersensitivity to aldicarb-induced paralysis, but this was less severe than what was observed for *ATXN3-CAG89* animals. These data suggest that the function of the GABAergic motoneurons, and perhaps their inhibitory signalling function, is impaired in mutant *ATXN3-CAG89* transgenics.

Additionally, we tracked the movement of wild-type N2 worms and both *ATXN3* transgenics for a period of 10 min on agar plates. We observed that *ATXN3-CAG89* worms had impaired motility phenotypes and explored less of their area compared with wild-type N2, and *ATXN3-CAG10* worms at days 1, 5 and 9 of adulthood (Fig. 2D). Overall, these data demonstrate that mutant

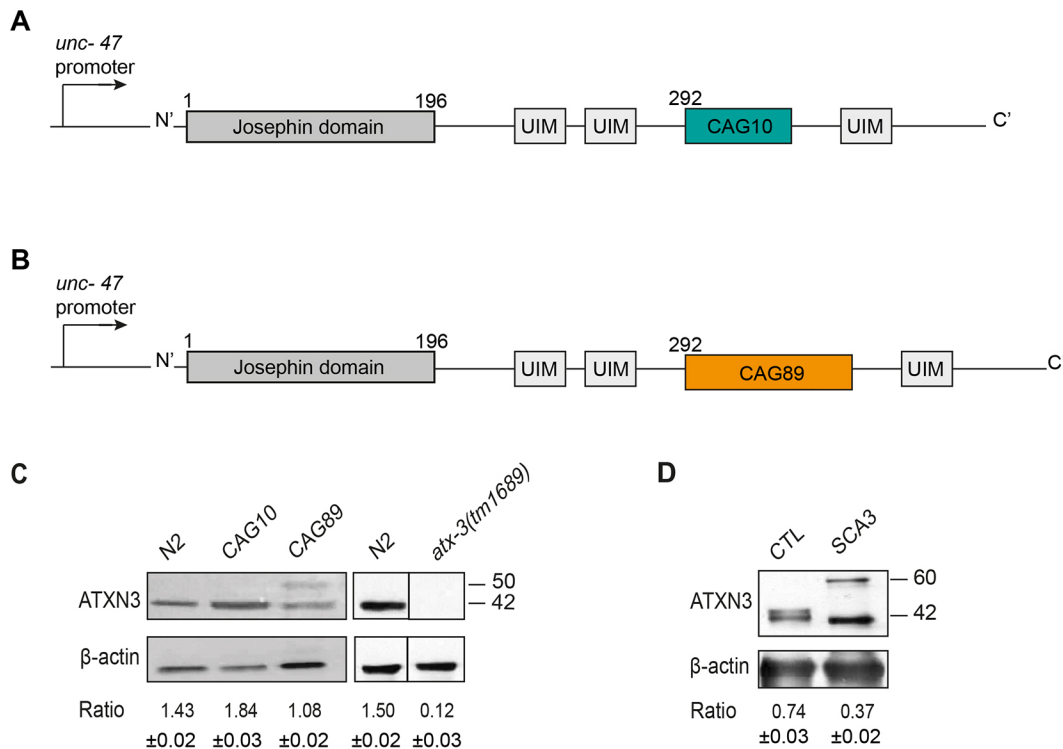


Fig. 1. Transgenic *C. elegans* ATXN3 model. (A) Full-length wild-type human ATXN3 containing 10 CAG trinucleotide repeat expansion or (B) full-length human ATXN3 with a polyglutamine expansion (CAG89) were expressed under the control of a *unc-47* promoter. CAG10/CAG89, polyglutamine sequences; UIM, interaction domains with ubiquitin. (C) Total protein levels for N2, *atx-3(tm1689)* and transgenic worms expressing ATXN3-CAG10 or mutant ATXN3-CAG89. Antibody detection revealed signals for transgenic and N2 wild-type worms, but no corresponding signal was detected in *atx-3(tm1689)* samples. Bands observed at ~42 kDa in size corresponding to full-length ATXN3 were observed in extracts from transgenic ATXN3-CAG10 worms, and a slightly larger band at ~50 kDa in size was observed for ATXN3-CAG89 samples. A band was observed in non-transgenic N2 worms, probably representing the endogenous ATX-3 protein. No band was observed in the *atx-3(tm1689)* deletion mutant. The *atx-3(tm1689)* western blots were done independently from the transgenic ATXN3 experiments. For the ATXN3-CAG89 lane, the ratio of ATXN3 to actin was made using the top band. (D) Total protein levels from cells derived from healthy (control; CTL) and MJD (SCA3) patients. Staining showed signals for both healthy and MJD patients, having an estimated molecular weight of 42 kDa and 60 kDa, respectively. For all experiments, actin staining was used as a loading control, and the expression ratio \pm s.e.m. of ATXN3 to actin was determined from three independent experiments. Representative western blots are shown.

ATXN3-CAG89 transgenic worms have increased neuromuscular dysfunction that advances in a progressive manner, leading to increased rates of paralysis compared with controls.

Mutant ATXN3-CAG89 causes progressive motoneuron degeneration

Many neurodegenerative diseases are characterized by neuronal dysfunction before degeneration (Saxena and Caroni, 2011). To determinate whether the progressive paralysis phenotype observed in ATXN3-CAG89 worms was accompanied by neurodegeneration, we crossed the transgenic lines with an integrated reporter, *unc-47p::mCherry*, expressing the red fluorescent protein mCherry in GABAergic motoneurons (Petrash et al., 2013). We observed a significant increase of gaps and/or breaks in motoneurons of ATXN3-CAG89 worms when compared with the wild-type *unc-47p::mCherry* and ATXN3-CAG10 transgenics at days 5 and 9 of adulthood (Fig. 2E,F). We did not observe neurodegeneration in young adult day 1 mutant ATXN3-CAG89 transgenic worms (Fig. S1B). These observations suggest a gradual decline of neuronal function that is correlated with age-dependent neurodegeneration as observed in diseases such as MJD.

We investigated whether endogenous *atx-3* contributed to motility and neurodegeneration phenotypes in our ATXN3-CAG89 transgenics. We observed that the rates of paralysis and neurodegeneration of *atx-3(tm1689)*; ATXN3-CAG89 animals was

indistinguishable from ATXN3-CAG89 controls, suggesting that *atx-3* does not contribute to ATXN3-CAG89 phenotypes (Fig. S1).

As ATXN3 and mCherry are both expressed under the same promoter (*unc-47*), we wondered whether transcription factor depletion could contribute to the motility phenotypes observed in our ATXN3-CAG89 transgenics. To investigate, we turned to a worm tracking system (*Wmicrotracker*; Phylum Tech) able to measure both automatically and simultaneously the movement of a population of worms placed in 96-well microtitre plates over several hours (Veriepe et al., 2015; Vaccaro et al., 2012a; Therrien and Parker, 2014; Schmeisser et al., 2017). The apparatus makes use of two infrared light beams crossing each microtitre well from top to bottom, and a detector determines how often the light rays are interrupted by worms moving in the well. Each interruption counts as a movement registered by the machine (Schmeisser et al., 2017). We observed no difference in overall movement between ATXN3-CAG89 and *unc-47p::mCherry*; ATXN3-CAG89 worms (Fig. S2). These data suggest that the addition of the *unc-47p::mCherry* transgene to ATXN3-CAG89 transgenics does not influence motility phenotypes.

Methylene Blue, salubrinal and guanabenz suppress paralysis and extend lifespan in ATXN3-CAG89 transgenics without affecting the expression of this transgene

Our group previously identified several small molecules, including Methylene Blue, salubrinal and guanabenz, that target the ER stress

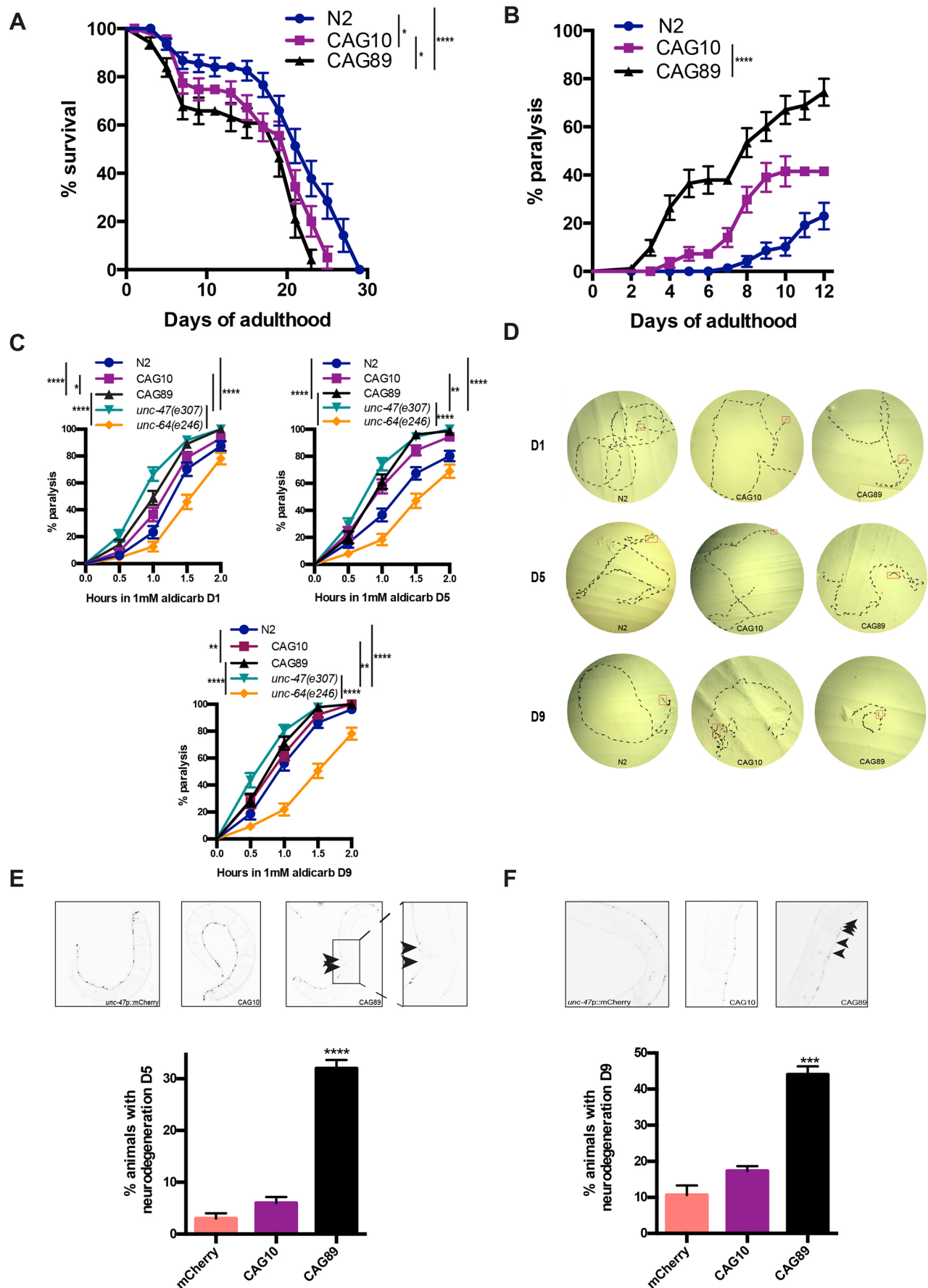


Fig. 2. Lifespan and neuronal phenotypes in *ATXN3* transgenics.

(A) *ATXN3-CAG89* worms had reduced lifespan compared with wild-type *ATXN3-CAG10* or N2 worms [$*P<0.05$ and $****P<0.0001$, respectively, by log-rank (Mantel–Cox) test; $n=300$ –360]. *ATXN3-CAG10* animals showed reduced lifespan compared with N2 wild-type worms [$*P<0.05$, by log-rank (Mantel–Cox) test; $n=300$ –360]. The experiment was repeated three times. (B) *CAG89* transgenics had a significantly higher paralysis phenotype compared with wild-type *ATXN3-CAG10* transgenics [$****P<0.0001$, by log-rank (Mantel–Cox) test; $n=270$ –300]. The experiment was repeated three times. (C) Cholinergic neuronal transmission was measured by determining the onset of paralysis induced by the cholinesterase inhibitor aldicarb. Adult day 1 *unc-47(e307)* and *ATXN3-CAG89* mutant strains showed a higher hypersensitive phenotype in the presence of the aldicarb-induced paralysis compared with wild-type N2, *ATXN3-CAG10* and *unc-64(e246)* worms [$****P<0.0001$ for *unc-47(e307)* mutant worms when compared with the controls, and $****P<0.0001$, $*P<0.05$ and $****P<0.0001$ for *ATXN3-CAG89* mutants compared with the controls, by log-rank (Mantel–Cox) test; $n=270$ –300]. Adult day 5 *unc-47(e307)* and *ATXN3-CAG89* worms also showed a higher hypersensitive phenotype in presence of the aldicarb-induced paralysis compared with wild-type N2, *ATXN3-CAG10* and *unc-64(e246)* worms [$****P<0.0001$, $**P<0.01$ and $****P<0.0001$ for *unc-47(e307)* mutants, respectively, compared with the controls, and $****P<0.0001$ for *ATXN3-CAG89* mutants when compared with wild-type N2 and *unc-64(e246)* worms, by log-rank (Mantel–Cox) test; $n=270$ –300]. A hypersensitive phenotype was observed at adult day 9 *unc-47(e307)* and *ATXN3-CAG89* mutant strains when compared with wild-type N2, *ATXN3-CAG10* and *unc-64(e246)* worms [$****P<0.0001$, $**P<0.01$ and $****P<0.0001$ for *unc-47(e307)* mutant worms when compared with the controls, respectively, and $**P<0.01$ and $****P<0.0001$ for *ATXN3-CAG89* mutants when compared with the wild-type N2 and *unc-64(e246)* worms, by log-rank (Mantel–Cox) test; $n=270$ –300]. The experiment was repeated three times. (D) Synchronized adult day 1, 5 and 9 worms were placed on NGM plates and photographed after 10 min of free movement. *ATXN3-CAG89* mutant worms showed defects in motility when compared with wild-type N2 and *ATXN3-CAG10* transgenic worms. (E,F) Representative photos of living, adult expressing wild-type *unc-47p::mCherry*, *unc-47p::mCherry*; *ATXN3-CAG10* and *unc-47p::mCherry*; *ATXN3-CAG89* transgenic worms at days 5 and 9 of adulthood. Images of the GABAergic motoneurons from entire *unc-47p::mCherry* and *unc-47p::mCherry*; *ATXN3-CAG10* worms were taken. Image of an entire *unc-47p::mCherry*; *ATXN3-CAG89* transgenic worm was taken and then zoomed in the panel on the right, representing a magnification of the area indicated. Increased incidences of gaps or breakages were observed in mutant *unc-47p::mCherry*; *ATXN3-CAG89* transgenics compared with wild-type *unc-47p::mCherry* and *unc-47p::mCherry*; *ATXN3-CAG10* controls. Quantification of neurodegeneration in transgenic worms at days 5 and 9 of adulthood. *ATXN3-CAG89* transgenics showed a significant increase of neurodegeneration compared with *unc-47p::mCherry* and *ATXN3-CAG10* controls ($****P<0.0001$ for day 5 of adulthood and $***P<0.001$ for adult day 9 worms, by Student's unpaired *t*-test; $n=100$ for each condition). These experiments were replicated three times.

response and were shown to have beneficial effects against mutant TDP-43 neuronal toxicity in models for ALS (Vaccaro et al., 2012a, 2013) and to have protective effects in models for hereditary spastic paraplegia (Julien et al., 2016). Thus, we wondered whether these compounds had neuroprotective activity against mutant *ATXN3-CAG89*. We tested these compounds and found that all three molecules suppressed the age-dependent paralysis phenotype caused by mutant *ATXN3-CAG89* (Fig. 3A–C), and extended the lifespan of these transgenic worms (Fig. 3D). Additionally, we wondered whether these compounds had any effect on the expression of *ATXN3-CAG89* transgenes, perhaps influencing paralysis and lifespan phenotypes. We confirmed that these compounds did not affect the expression of *ATXN3-CAG89* transgenes by western blotting with a human specific anti-*ATXN3* antibody (Fig. 3E).

To confirm the neuroprotective activity of these molecules with a separate approach, we turned to our automated assay measuring the movement of *C. elegans* grown in liquid culture (Veriepe et al.,

2015; Vaccaro et al., 2012a; Therrien and Parker, 2014). We observed that *ATXN3-CAG89* animals treated with Methylene Blue, salubrinal or guanabenz had increased motility compared with untreated controls (Fig. 4). These data suggest that molecules regulating the ER stress response can attenuate neuronal dysfunction caused by mutant *ATXN3-CAG89*.

Small molecules rescue neurodegeneration in *ATXN3-CAG89* transgenics

After observing that Methylene Blue, salubrinal or guanabenz suppressed mutant *ATXN3-CAG89*-induced paralysis, we examined whether these compounds had protective effects against motoneuron degeneration. Using the *unc-47p::mCherry*; *ATXN3-CAG89* strain, we visualized the GABAergic motoneurons *in vivo* in day 5 adults and observed a significant decrease of neurodegeneration for worms when treated with any of the three compounds (Fig. 5). These data demonstrate that chemical manipulation of ER stress mechanisms protects neurons against mutant *ATXN3* toxicity.

Methylene Blue, salubrinal and guanabenz prevent the oxidative stress induced by *ATXN3-CAG89* transgenics

We wondered whether one mechanism associated with mutant *ATXN3-CAG89* toxicity involved elevated levels of oxidative stress, as we have previously observed in other models of neuronal proteotoxicity (Vaccaro et al., 2013, 2012a). Global oxidative stress can be detected by staining worms with the fluorescent dye 2',7'-dichlorofluorescein diacetate (DCF-DA), and we observed increased fluorescence in *ATXN3-CAG89* transgenics compared with wild-type N2 controls and *ATXN3-CAG10* transgenics (Fig. 6A–C).

Our previous work suggests that oxidative stress might be linked with activation of the unfolded protein response in the ER (Julien et al., 2016; Vaccaro et al., 2013). Furthermore, small molecule-mediated reduction of the ER stress response was likewise correlated with decreased oxidative stress levels in *C. elegans* proteotoxicity models. We observed that treatment of *ATXN3-CAG89* transgenics with Methylene Blue, guanabenz or salubrinal reduced the fluorescence from DCF-DA staining (Fig. 6D–G). These data suggest that the ER stress response might be involved in neuronal toxicity caused by mutant *ATXN3-CAG89*.

Rescue of ER stress response by Methylene Blue, salubrinal and guanabenz in *ATXN3-CAG89* transgenic worms

After observing high levels of oxidative stress in *ATXN3-CAG89* transgenics, we wanted to test directly for the involvement of the ER stress response. *hsp-4* encodes a widely expressed, protective Hsp70/BiP protein induced by ER stress that can be monitored with a transgenic, transcriptional *hsp-4::GFP* reporter that shows strong fluorescence in the intestine and spermatheca (Urano et al., 2002). We crossed the *ATXN3* transgenics with the *hsp-4::GFP* reporter and observed increased fluorescence in *ATXN3-CAG89*; *hsp-4::GFP* animals compared with *ATXN3-CAG10*; *hsp-4::GFP* or *hsp-4::GFP* controls (Fig. 7A, top panels). We recently showed that Methylene Blue, guanabenz and salubrinal rescue the ER stress response in multiple models for another neurological disorder, hereditary spastic paraplegias (Julien et al., 2016). Based on this finding, we examined whether any of these compounds were able to prevent the ER stress response caused by *ATXN3-CAG89* transgenics. We found that all three compounds reduced fluorescence of the ER stress *hsp-4::GFP* reporter transgene in *ATXN3-CAG89* transgenics (Fig. 7A–D). A significant reduction of the ER stress was also observed in the *ATXN3-CAG10* transgenic worms when treated with

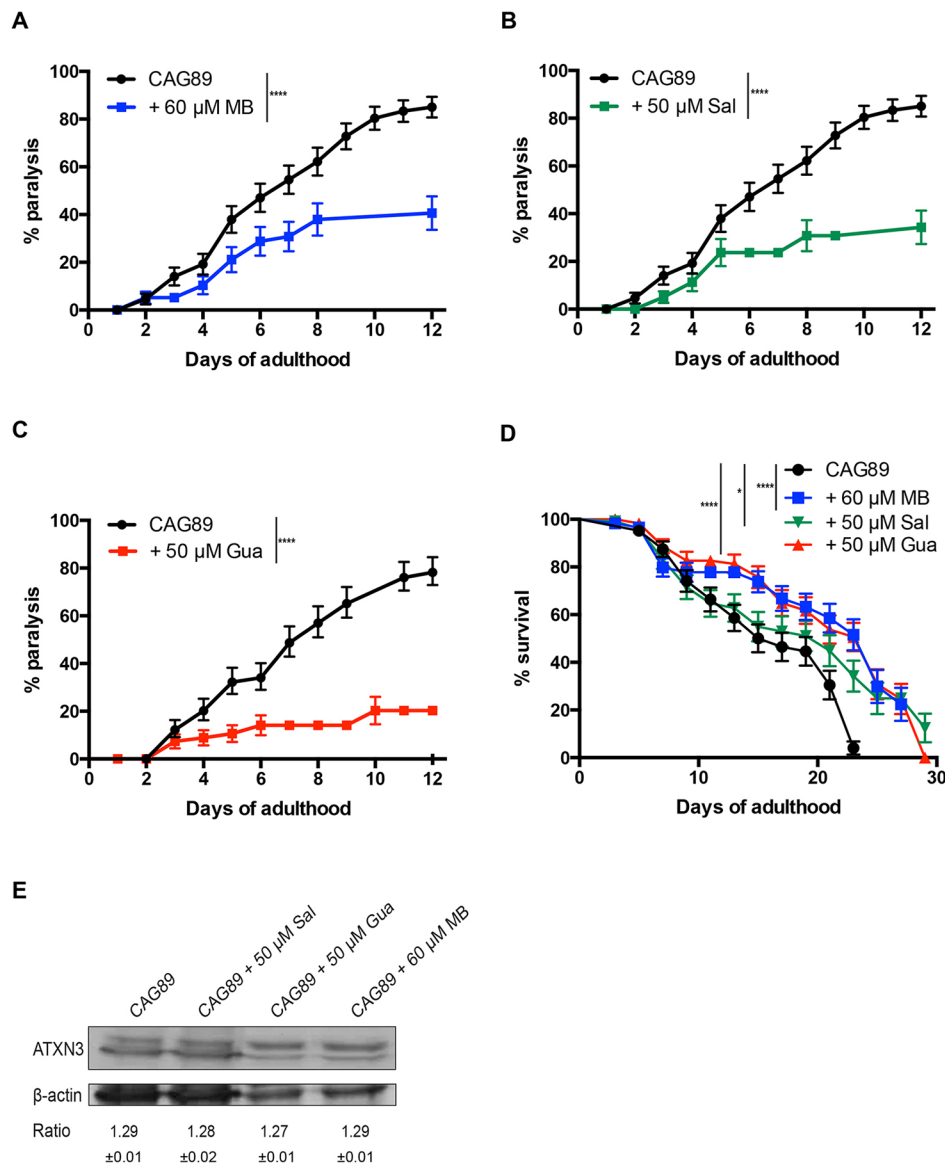


Fig. 3. Methylene Blue, salubrinal or guanabenz suppresses paralysis during ageing and extends lifespan in *ATXN3-CAG89* worms without affecting the expression level of this transgene.

(A-C) The motor defect phenotype observed in *ATXN3-CAG89* worms was significantly decreased in the presence of 60 μ M MB (**** P <0.0001), 50 μ M Sal (**** P <0.0001) or 50 μ M Gua (**** P <0.0001) [by log-rank (Mantel-Cox) test; n =270-300]. This experiment was replicated three times. (D) *ATXN3-CAG89* worms showed an increase lifespan in the presence of 60 μ M MB (**** P <0.0001), 50 μ M Sal (* P <0.05) or 50 μ M Gua (**** P <0.0001) [by log-rank (Mantel-Cox) test; n =300-360]. This experiment was replicated three times. (E) Total protein levels for transgenic worms expressing mutant *ATXN3-CAG89* with and without exposure to Sal, Gua or MB. Antibody detection revealed signals for all four conditions. No differences in expression were observed between the untreated and treated transgenic worms. Actin staining was used as a loading control, and the expression ratio \pm s.e.m. of *ATXN3* to actin was determined from three independent experiments. Representative western blots are shown. Gua, guanabenz; MB, Methylene Blue; Sal, salubrinal.

the compounds. This is consistent with the fact that *ATXN3-CAG10* transgenics have motility and lifespan phenotypes intermediate to N2 worms and *ATXN3-CAG89* transgenics. We observed a significant induction of the GFP signal in *hsp-4::GFP* worms when treated with Methylene Blue and salubrinal, suggesting that these molecules might act by stimulating an early ER stress response outcome that might be neuroprotective in the context of *ATXN3* transgenics, ultimately resulting in lower proteotoxicity followed by decreased ER stress overall. These data suggest that small molecule interventions centred on the ER stress response protect against mutant *ATXN3* toxicity.

If stress within the ER persists, and it is not resolved by the early protective ER unfolded protein response (UPR^{ER}) pathways, this can stimulate the clearance of misfolded proteins from the ER through ER-associated degradation (ERAD). The processing of misfolded proteins by ERAD is a redox-intensive process that requires the ER oxidoreductase *ero-1*/ERO1, the activity of which can result in the production of peroxides and, consequently, increased reactive oxygen species (Harding et al., 2003). Thus, impairing *ero-1*/ERO1 activity disrupts the processing of proteins, along with the generation of peroxides and associated oxidative stress (Harding et al., 2003).

Therefore, we predicted that knockdown of *ero-1* by RNAi could reduce the amount of oxidative stress observed in our *ATXN3-CAG89* transgenics worms. We observed that *ATXN3-CAG89* mutant worms stained with DCF-DA in the presence of *ero-1*(RNAi) showed a significant decrease of fluorescence compared with the empty vector RNAi controls (Fig. 7E). These data suggest that the oxidative stress observed in our *ATXN3-CAG89* transgenic mutant worms might originate in the ER and is dependent on the activity of *ero-1*.

Chemical-genetic approach analysis for the UPR^{ER} pathways

ER stress leads to activation of the UPR by three main signalling branches, resulting in an upregulation of chaperone proteins and a general arrest of protein translation (Walker and Atkin, 2011). Based on our data demonstrating an activation of ER stress in *ATXN3-CAG89* mutants, along with a reduction of this stress by UPR^{ER}-associated compounds (Fig. 7), we wondered whether these compounds required any specific UPR^{ER} branches for their neuroprotective activities. To identify the mechanisms related to each compound, we opted for a genetic approach using mutants against key components of two branches of the UPR^{ER} pathways, such as *atf-6*/ATF6, *pek-1*/PERK, and RNAi for *ire-1*/IRE1.

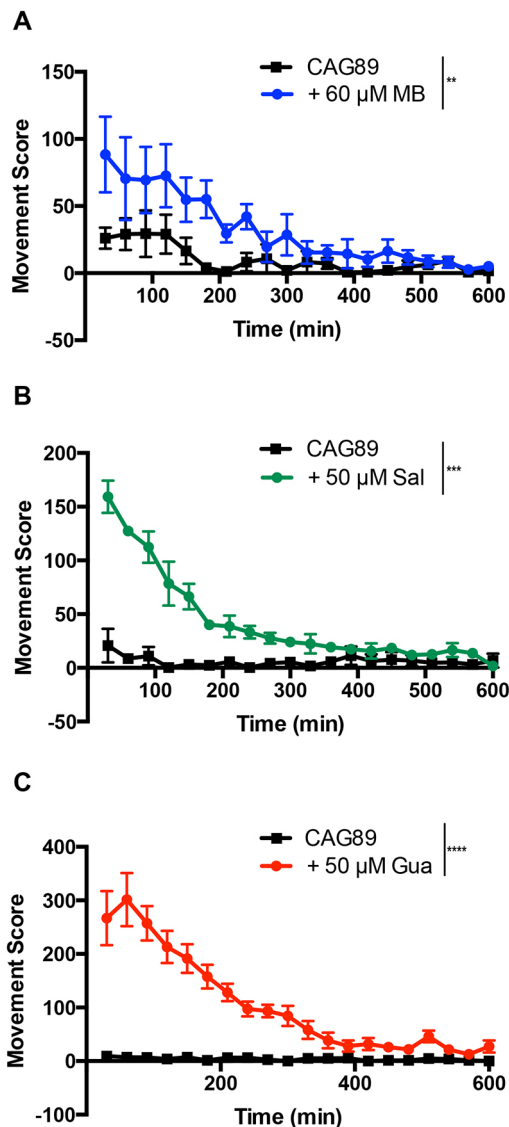


Fig. 4. Methylene Blue, salubrin or guanabenz suppresses acute paralysis in ATXN3-CAG89 transgenics. The swimming activity of ATXN3-CAG89 worms was scored for a period of 10 h, and treatment with (A) 60 μM MB (** $P < 0.01$), (B) 50 μM Sal (*** $P < 0.001$) or (C) 50 μM Gua (**** $P < 0.0001$) (by Student's unpaired *t*-test) significantly rescued the impaired movement phenotype of ATXN3-CAG89 worms. This experiment was done three times. Gua, guanabenz; MB, Methylene Blue; Sal, salubrin.

We investigated the contribution of the *pek-1*/PERK pathway with the deletion mutant *pek-1(ok275)*. We observed that the rescuing activity of guanabenz was completely dependent on *pek-1*. Methylene Blue continued to suppress paralysis in the absence of *pek-1*, suggesting that this compound does not require the *pek-1*/PERK branch of the UPR^{ER}. Concerning salubrin, this compound was partly dependent on *pek-1*, because we observed a reduced ability to suppress paralysis in ATXN3-CAG89; *pek-1(ok275)* worms (Fig. 8A).

We examined the neuroprotective activity of *atf-6* using *atf-6(ok551)* mutant worms. We observed that *atf-6* was not required for the neuroprotective activity of Methylene Blue and salubrin, because these compounds maintained their ability to suppress paralysis in ATXN3-CAG89; *atf-6(ok551)* mutants. However, we observed that guanabenz failed to suppress the paralysis in ATXN3-CAG89

mutants when crossed with *atf-6* loss-of-function mutants, confirming dependence on the *atf-6* branch of the UPR^{ER} (Fig. 8B).

To investigate the role of *ire-1* in neuroprotection, we used RNAi against *ire-1(zc14)*. We observed that the rescuing activity of guanabenz was completely dependent on *ire-1*, and Methylene Blue showed a partial dependence on this branch of the UPR^{ER}. However, salubrin showed no dependence on this pathway, as this compound continued to suppress the paralysis in *ire-1*(RNAi) worms (Fig. 8C). These data suggest that the three chemical compounds use distinct, or possibly overlapping, branches of the UPR^{ER} to achieve neuroprotection against CAG-mediated proteotoxicity.

Small molecule suppression of ATXN3-CAG89 aggregation

As ATXN3 has been observed to form protein aggregates in several models, including *C. elegans*, we wondered whether our transgenics displayed similar aggregation phenotypes (Teixeira-Castro et al., 2015, 2011; Koch et al., 2011; Breuer et al., 2010). To determine whether ATXN3 proteins could be detected *in vivo*, we fixed whole ATXN3-CAG10 and ATXN3-CAG89 transgenics and stained them with a human ATXN3 antibody. We detected ATXN3 protein in the motoneurons of ATXN3 transgenics (Fig. 9A). Our cursory visual examination suggested a more intense puncta signal in ATXN3-CAG89 transgenics that might reflect increased aggregation potential of ATXN3-CAG89 protein compared with ATXN3-CAG10.

We investigated further using a biochemical assay to detect protein aggregation. Homogenized protein extracts from transgenic worms were separated into supernatant (detergent soluble) and pellet (detergent insoluble). Dot blotting the ATXN3-CAG89 transgenic mutants with human ATXN3 antibody showed a high accumulation of the ATXN3-CAG89 in the pelleted, insoluble fraction, when compared with ATXN3-CAG10 and N2 wild-type worms (Fig. 9B). We then investigated whether Methylene Blue, salubrin and guanabenz were able to reduce the aggregation observed in our ATXN3-CAG89 transgenics. We observed a significant decrease of aggregation in ATXN3-CAG89 worms when treated with these three compounds, and noted that guanabenz was especially potent in reducing protein aggregation (Fig. 9B,C). These data suggest neuroprotective roles for Methylene Blue, salubrin and guanabenz in reducing mutant ATXN3 aggregation.

DISCUSSION

We introduce new *C. elegans* models for investigating mechanisms of motoneuron toxicity caused by a polyglutamine expansion in ATXN3. To model human disease, we expressed full-length human ATXN3 without additional tags, because the inclusion of tags can mask or enhance the phenotypes of wild-type and mutant proteins (Catoire et al., 2008; Wang et al., 2009). We engineered strains expressing ATXN3 in the animal's 26 GABAergic neurons, because impaired activity of these motoneurons can lead to easily identifiable motility phenotypes useful for screening purposes (McIntire et al., 1997, 1993). Additionally, MJD disease is in part associated with dysfunction of motoneurons (França et al., 2008; Kanai and Kuwabara, 2009; Pinto and De Carvalho, 2008; Rub et al., 2002). Furthermore, we have previously constructed neurodegeneration models based on the expression of human disease proteins in these same GABAergic motoneurons and found that the transgenic models provide robust phenotypes for experimentation, as we have previously demonstrated in our ALS models (Vaccaro et al., 2012a). Lastly, *C. elegans* has an ATXN3 orthologue, ATX-3, that shares many cellular functions (Kawaguchi

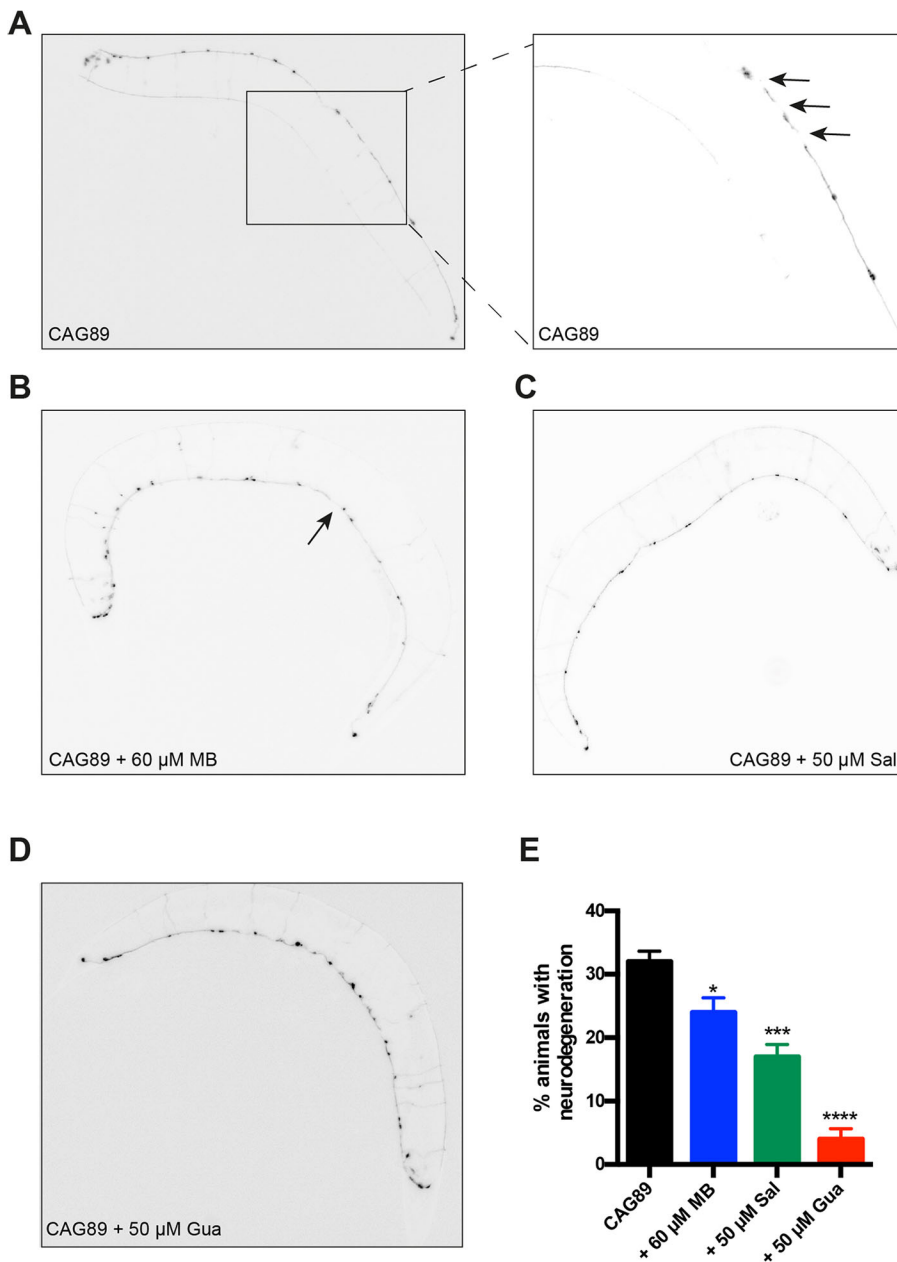


Fig. 5. Rescue of motoneuron degeneration by small molecules in ATXN3-CAG89 transgenics. Shown are representative photos of living, adult *unc-47p::mCherry*; ATXN3-CAG89 transgenics at day 5 of adulthood with or without compounds. Images are black and white, photo-reversed to aid visualization of neurons. (A) Image of degenerating GABAergic motoneurons from an entire ATXN3-CAG89 transgenic. The panel on the right is a magnification of the area indicated by the rectangle. Arrows indicate gaps or breaks along neuronal processes. Rescue of neurodegeneration was observed in ATXN3-CAG89 worms in the presence of (B) 60 μ M MB, (C) 50 μ M Sal or (D) 50 μ M Gua. (E) Quantification of neurodegeneration in transgenic ATXN3-CAG89 worms at day 5 of adulthood. Significant rescue of the neurodegeneration morphology was observed in ATXN3-CAG89 transgenics when treated with 60 μ M MB (* P <0.05), 50 μ M Sal (*** P <0.001) or 50 μ M Gua (**** P <0.0001) (by Student's unpaired *t*-test, n =100 for each condition). These experiments were repeated three times. Gua, guanabenz; MB, Methylene Blue; Sal, salubrinal.

et al., 1994; Rodrigues et al., 2007; Piano et al., 2002), which perhaps extend to the nervous system, making the worm an appropriate model for studying conserved pathophysiological mechanisms of MJD.

ATXN3-CAG89 transgenic worms showed a progressive age-dependent paralysis, and reduced lifespan phenotypes compared with wild-type ATXN3-CAG10 transgenics. The fact that we observed a decrease of lifespan resulting from the expression of ATXN3 transgenes in GABAergic motoneurons suggests that there might be some sort of communication from the nervous system to the rest of the organism that negatively modifies health. We and others have observed that cellular stress originating in specific neuronal populations can affect organism-wide stress mechanisms that in turn can affect lifespan (Veriepe et al., 2015; Vaccaro et al., 2012c; Taylor and Dillin, 2013; van Oosten-Hawle et al., 2013). Future studies will help to elucidate how the neuronal expression of ATXN3 regulates lifespan.

Consistent with the reduced motility observed in ATXN3-CAG89 transgenics, we also observed significant neurodegeneration in ATXN3-CAG89 transgenics compared with ATXN3-CAG10 controls. These data demonstrate that the ATXN3-CAG89 transgenics produce phenotypes distinct from wild-type ATXN3-CAG10 and that these mutant animals might be suitable for modifier screening. Our western blotting experiments (Fig. 1C) raise the possibility that the expression of ATXN3-CAG89 could decrease the expression of the endogenous *C. elegans atx-3* gene, perhaps accounting for some of the negative phenotypes observed in ATXN3-CAG89 transgenics. We think this is unlikely because the western blotting data show that the level of endogenous ATX-3 in non-transgenic N2 worms (ratio 1.43) is lower than that of ATXN3-CAG10 controls (ratio 1.84), yet N2 worms do not have motility defects or paralysis phenotypes at a rate higher than the ATXN3-CAG10 transgenics. Furthermore, as we suspect that the anti-ATXN3 antibody detects ATX-3 and ATXN3, it is difficult to conclude

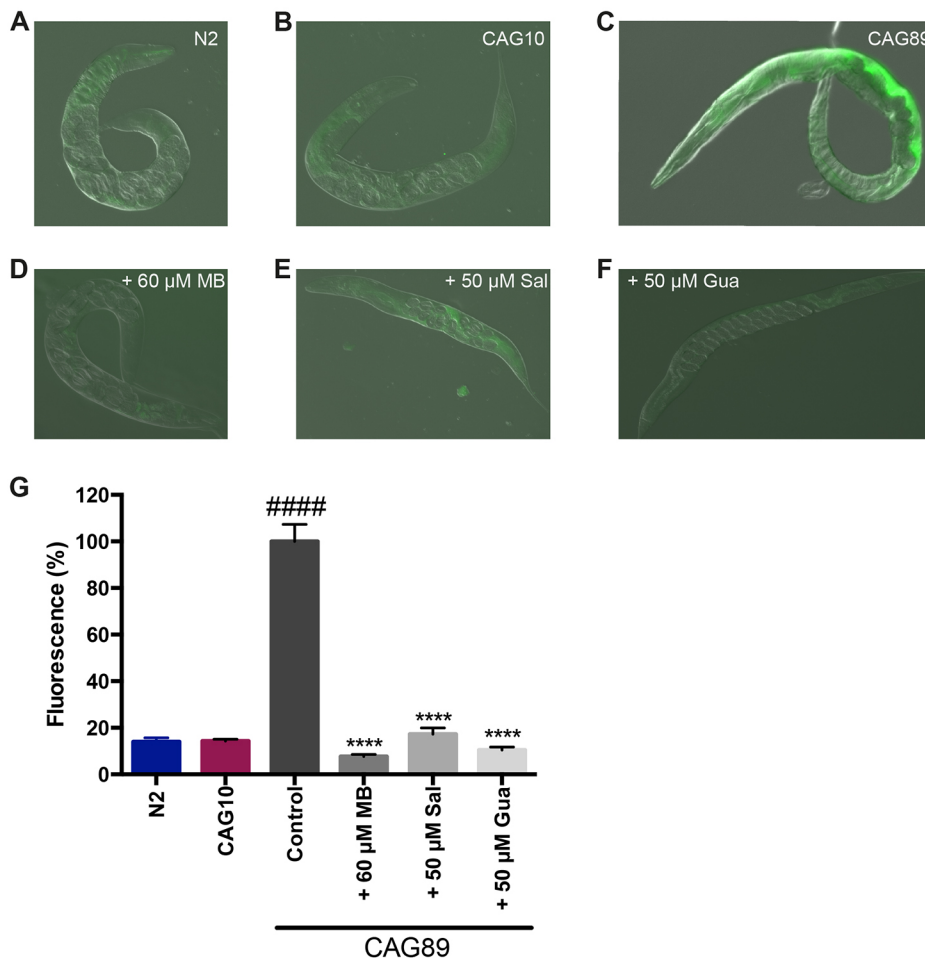


Fig. 6. Reduction of oxidative stress in *ATXN3-CAG89* transgenics by Methylene Blue, guanabenz or salubrinal. Shown are representative photos of living, adult (A) wild-type N2 worms and (B) wild-type *ATXN3-CAG10* and (C) mutant *ATXN3-CAG89* transgenics at day 2 of adulthood in the presence of the oxidative stress marker, 2',7'-dichlorofluorescein diacetate (DCF-DA). Increased fluorescence is observed in the (C) *ATXN3-CAG89* transgenic worms. (D-F) *ATXN3-CAG89* transgenics stained with DCF-DA showed decreased fluorescence after treatment with (D) 60 μ M MB, (E) 50 μ M Sal or (F) 50 μ M Gua. (G) Quantification of fluorescence in N2 controls, *ATXN3-CAG10* or *ATXN3-CAG89* transgenics stained with DCF-DA. *ATXN3-CAG89* transgenics showed increased fluorescence compared with N2 or *ATXN3-CAG10* worms (##### P <0.0001). *ATXN3-CAG89* transgenics had less fluorescence when treated with 60 μ M MB, 50 μ M Sal or 50 μ M Gua in the presence of DCF-DA compared with untreated CAG89 controls (**** P <0.0001) (Student's unpaired *t*-tests, n =17-25 for each condition). This experiment was repeated three times. Gua, guanabenz; MB, Methylene Blue; Sal, salubrinal.

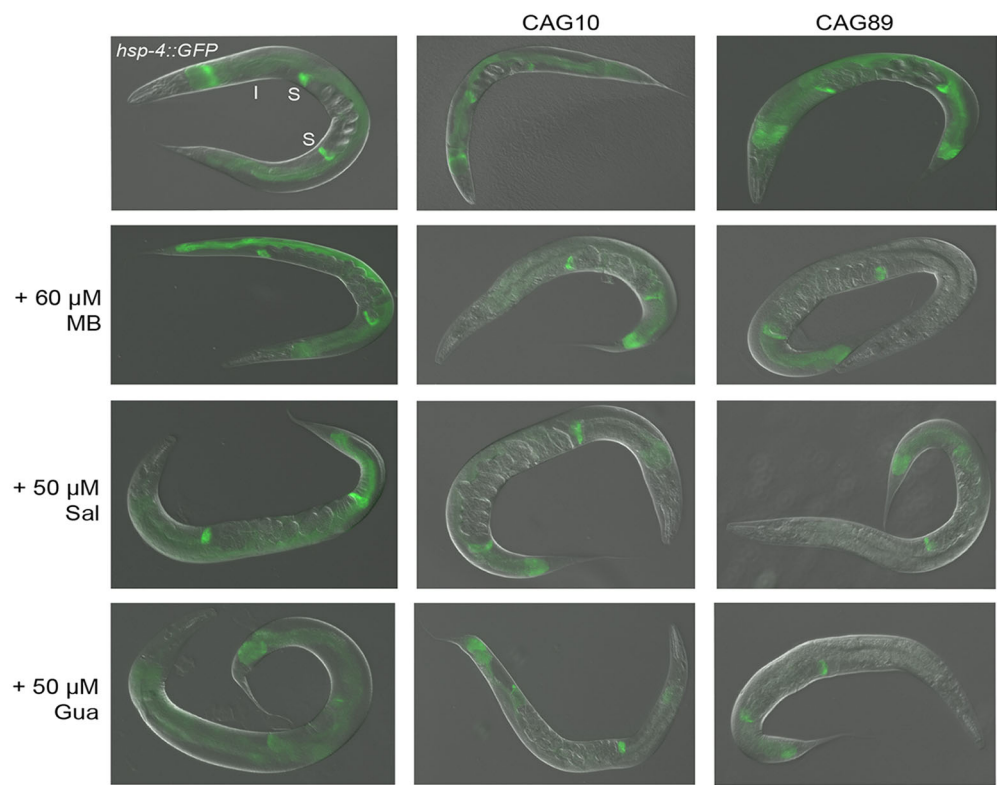
definitively that the levels of endogenous ATX-3 are meaningfully different in the respective strains. Future investigations with more specific antibodies might help to resolve this issue.

Several transgenic *C. elegans* *ATXN3* models have been reported, consisting of full-length or fragments of *ATXN3*, a variety of CAG repeat lengths, with the protein often fused to a fluorescent marker, and high copy expression in body wall muscle cells or the entire nervous system (Khan et al., 2006; Bonanomi et al., 2014; Teixeira-Castro et al., 2011; Christie et al., 2014). The novelty of our approach is that we have expressed full-length, untagged human *ATXN3* at low levels based on MoSCi transposon-mediated single copy insertion where transgenics express only two copies of the *ATXN3* transgene. Furthermore, these transgenics have been engineered to express wild-type or mutant *ATXN3* in a subset of the worm's motoneurons, resulting in strong phenotypes from a small number of cells. We believe this approach will aid drug screening, where any particular compound might need to be active in only a small number of neurons to allow for detection of suppression. Furthermore, motoneuron degeneration has been associated with MJD (França et al., 2008; McIntire et al., 1993, 1997; Pinto and De Carvalho, 2008; Kanai and Kuwabara, 2009; Rub et al., 2002).

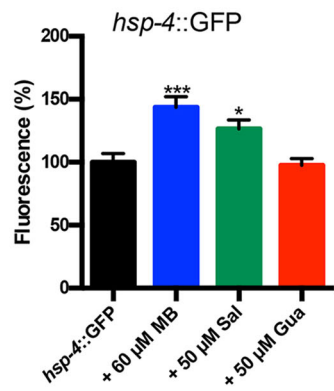
To explore the potential of our *ATXN3* transgenics in chemical modifier screens, we tested whether we could suppress mutant *ATXN3-CAG89* phenotypes with known neuroprotective compounds. Considering the evidence linking *ATXN3* containing expanded CAG repeats to ER stress (Rodrigues et al., 2011; Evers

et al., 2014; Costa and Paulson, 2012; Matos et al., 2011; Reina et al., 2010), and our previous findings connecting ER stress to other neurodegenerative diseases (Vaccaro et al., 2012a, 2013; Julien et al., 2016), we investigated whether pharmacological interventions centred on ER stress could protect against mutant *ATXN3-CAG89* toxicity. We focused on three compounds, guanabenz, salubrinal and Methylene Blue, for their known neuroprotective activity and their roles as ER stress modulators (Matos et al., 2011; Rodrigues et al., 2011; Vaccaro et al., 2013, 2012a). Encouragingly, we observed that the three compounds rescued motility defects, reduced lifespan, neurodegeneration and aggregation in animals expressing mutant *ATXN3-CAG89*. Moreover, these three compounds were also able to prevent the oxidative stress and the ER stress response induced in *ATXN3-CAG89* transgenics. Of the three compounds tested, we observed that guanabenz was the most effective at suppressing motility defects, neurodegeneration and protein aggregation phenotypes in *ATXN3-CAG89* animals. Finally, we identified the branches of the UPR^{ER} pathways essential for neuroprotection against mutant *ATXN3*. It is worth noting that mutations in individual UPR^{ER} genes (*ire-1*, *pek-1* or *atf-6*) did not exacerbate *ATXN3-CAG89* toxicity, suggesting that there might be redundancy between the pathways. This is consistent with the notion that the compounds tested activate the UPR^{ER} pathway to reduce *ATXN3-CAG89* toxicity. Thus, disabling individual genes blocks the activity of some molecules and not others, and helps to define the genetic requirements for neuroprotection by small molecules. However, we do predict that a triple mutant strain (*ire-1*, *pek-1* and *atf-6*) would

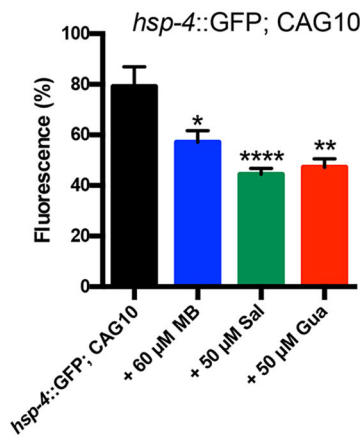
A



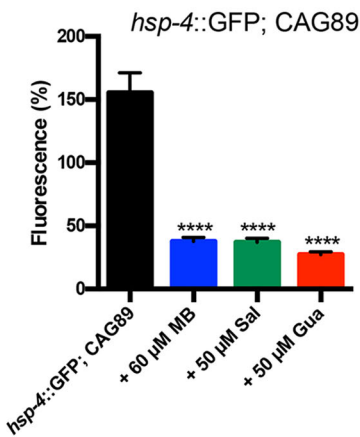
B



C



D



E

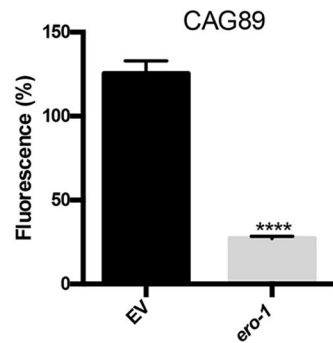
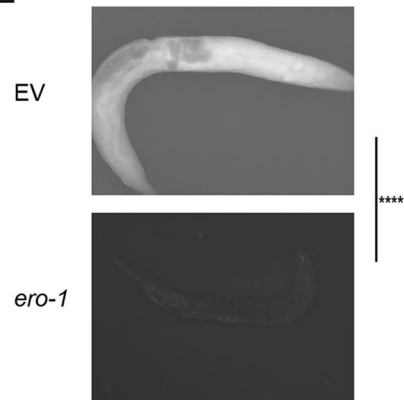


Fig. 7. See next page for legend.

Fig. 7. Methylene Blue, guanabenz and salubrinal rescue the ER stress response in *ATXN3-CAG89* transgenic worms. (A) Shown are representative photos of living, adult *hsp-4::GFP*; *hsp-4::GFP*; *ATXN3-CAG10* and *hsp-4::GFP*; *ATXN3-CAG89* transgenics at day 1 of adulthood. The *hsp-4::GFP*; *ATXN3-CAG89* transgenics show increased GFP expression compared with *hsp-4::GFP*, or *hsp-4::GFP*; *ATXN3-CAG10* controls (top panels). Treatment with 60 μ M MB, 50 μ M Sal or 50 μ M Gua reduces the fluorescence of *hsp-4::GFP*; *ATXN3-CAG89* to control levels. The *hsp-4::GFP* reporter shows increased fluorescence in the intestine (I) and spermatheca (S) of adult animals. (B–D) Quantification of fluorescence of transgenics with or without treatment with compounds. Increased fluorescence was observed in *hsp-4::GFP* worms when treated with 60 μ M MB (*** P <0.001) or 50 μ M Sal (* P <0.05) (Student's unpaired t -tests, n =17–25 for each condition). Fluorescence was decreased in *hsp-4::GFP*; *ATXN3-CAG10* transgenic worms when treated with 60 μ M MB (* P <0.05), 50 μ M Sal (**** P <0.0001) or 50 μ M Gua (** P <0.01) (Student's unpaired t -tests, n =17–25 for each condition). However, the decreased fluorescence observed was even more significant in *hsp-4::GFP*; *ATXN3-CAG89* mutants when treated with 60 μ M MB, 50 μ M Sal or 50 μ M Gua (**** P <0.0001) (Student's unpaired t -tests, n =17–25 for each condition). These experiments were replicated three times. (E) Shown are representative photos of living, adult day 2 *ATXN3-CAG89* transgenics fed with *E. coli* containing an empty vector (EV) or expressing dsRNA against *ero-1*. *ATXN3-CAG89* mutant worms showed a high level of fluorescence when stained with 2',7'-dichlorofluorescein diacetate (DCF-DA) and a significant decrease of this fluorescence when grown in the presence of *ero-1* RNAi. Quantification of fluorescence of *ATXN3-CAG89* mutant worms on EV or *ero-1* RNAi. A significant decrease of fluorescence of *ATXN3-CAG89* mutants was observed in the presence of *ero-1* RNAi when compared with EV (**** P <0.0001) (Student's unpaired t -tests, n =17–25 for each condition). This experiment was repeated three times. Gua, guanabenz; MB, Methylene Blue; Sal, salubrinal.

enhance *ATXN3-CAG89* toxicity and block the rescuing activity of all molecules tested here.

Additional studies are required to extend these findings to mammalian models of MJD. However, from a practical perspective, given that guanabenz has US Food and Drug Administration approval and is being tested in a clinical trial for multiple sclerosis, it could be translated rapidly into clinical settings for MJD.

Future studies will make use of unbiased drug screen approaches to identify additional neuroprotective molecules. The novelty of this approach relies on rapidly identifying molecules that restore movement in *ATXN3-CAG89* transgenics, followed by systematic characterization of lifespan, neurodegeneration and aggregation phenotypes. Our *C. elegans* *ATXN3* strains might serve as the initial step of an *in vivo* drug discovery and development pipeline for MJD and other polyglutamine diseases.

MATERIALS AND METHODS

Nematode strains

Standard methods of culturing and handling worms were used (Stiernagle, 2006). Worms were maintained on standard nematode growth media (NGM) plates streaked with OP50 *Escherichia coli*. All strains were scored at 20°C. Strains used for this study were as follows: N2, *atx-3(tm1689)*, *unc-47(e307)*, *unc-64(e246)*, *zcls4[hsp-4::GFP]*, *atf-6(ok551)* and *pek-1(ok275)*; all obtained from the *C. elegans* Genetics Center (University of Minnesota, Minneapolis).

Transgenic *ATXN3* worms and plasmid constructs

Human cDNAs for wild-type and mutant *ATXN3* were obtained from Dr Guy Rouleau (Montreal Neurological Institute and Hospital, McGill University). The cDNAs were amplified by PCR and cloned into the Gateway vector pDONR221 following the manufacturer's protocol (Invitrogen). Multisite Gateway recombination was performed with the pDONR *ATXN3* clones along with clones containing the *unc-47* promoter (obtained from Dr Erik Jorgensen, University of Utah), the *unc-54* 3'UTR plasmid pCM5.37 (obtained from Dr Geraldine Seydoux, Johns Hopkins; Addgene plasmid 17253) and the destination vector pCFJ150 to create *unc-47p::mCherry*;

ATXN3-CAG10 and *unc-47p::mCherry*; *ATXN3-CAG89* expression vectors. Transgenic lines were created by microinjection of *unc-119(ed3)* worms and screened for MoSCi transposon-mediated single copy insertion of the desired transgene. Several lines were isolated for each transgene of interest, and those showing similar behaviour, transgene expression levels and molecular profiles were outcrossed and kept for further analysis. The strains used in this study include the following: XQ350 *unc-119(ed3)*; tTi5605mosII; *xqls350(unc-47p::ATXN3-CAG10; unc-119(+))*, and XQ351 *unc-119(ed3)*; tTi5605mosII; *xqls351(unc-47p::ATXN3-CAG89; unc-119(+))*.

Age-synchronized populations

To obtain an age-synchronized population of worms, ~8–10 adult hermaphrodites were placed on 10 NGM plates for 3–4 days and kept at 20°C. Then, once the plates contained a large number of adult worms, they were collected with M9 buffer (1 M KH₂PO₄, 1 M Na₂HPO₄, 1 M NaCl and 1 M MgSO₄) and centrifuged at 3,250 g (A-4-81 Rotor) for 4 min at 4°C. After centrifugation, 3 ml of the supernatant was taken and replaced with 3 ml of a mix solution containing NaOH 5 M and bleach (1:2). This was vortexed for 10 min with a high intensity to degrade the worms, leaving a pellet containing only eggs. The pellet was washed four times with M9 buffer and centrifuged at 3,250 g (A-4-81 Rotor) for 4 min at 4°C. The pellet was transferred onto NGM plates without bacteria and kept overnight at 20°C. The next day, L1 worms were transferred using M9 buffer onto plates streaked with OP50 *E. coli* and kept at 20°C.

Paralysis assays on solid media

Worms expressing *ATXN3-CAG10*, *ATXN3-CAG89*, *unc-47p::mCherry*; *ATXN3-CAG10* and *unc-47p::mCherry*; *ATXN3-CAG89* were scored for paralysis from adult day 1 to adult day 12. Briefly, 30–40 L4 worms (obtained via synchronization) were transferred onto NGM plates and from adult day 1 to adult day 12, were scored as paralysed if they failed to move after being prodded with a worm pick. Worms were scored as dead if they were unable to respond to tactile head stimulus. They were transferred to fresh plates every 2 days until the cessation of progeny production. All experiments were conducted at 20°C, and each condition was done in triplicates with 30–40 worms per plate.

Lifespan assays

Approximately 40 L4 worms (obtained via synchronization) were transferred using M9 buffer on new NGM plates and tested daily from adult day 1 until death. Worms were transferred to fresh plates every 2 days until the cessation of progeny production. Worms were scored as dead if they failed to respond to tactile stimulus and showed no spontaneous movement or response when prodded. Dead worms displaying internally hatched progeny or extruded gonads or worms that crawled off the plate were excluded. The transgenic *ATXN3* strains were compared with wild-type worms (N2). All experiments were conducted at 20°C, and each condition was done in triplicates with 40 worms per plate.

Aldicarb tests

To evaluate synaptic transmission, synchronized worms were grown on NGM plates until adult day 1, 5 and 9. They were then transferred onto NGM plates plus 1 mM aldicarb. Paralysis was scored every 30 min for 2 h on aldicarb plates. Worms were counted as paralysed if they failed to move upon prodding with a worm pick. All experiments were conducted at 20°C. For each strain, the test was done in triplicates with 30 worms per plate in three independent replicates.

Tracking the movement on solid media

Synchronized adult day 1, 5 and 9 worms were placed on NGM plates for 10 min. Their movement tracking was filmed and photographed using a 12MP Camera installed on a standard laboratory microscope.

RNAi experiments

Synchronized L1 worms were transferred onto NGM plates enriched with 1 mM isopropyl- β -D-thiogalactopyranoside (IPTG). RNAi-treated *ATXN3-CAG89* worms were fed with *E. coli* containing an empty vector (EV) or expressing dsRNA against *ero-1* (Y105E8B.8) or *ire-1* (C41C4.4).

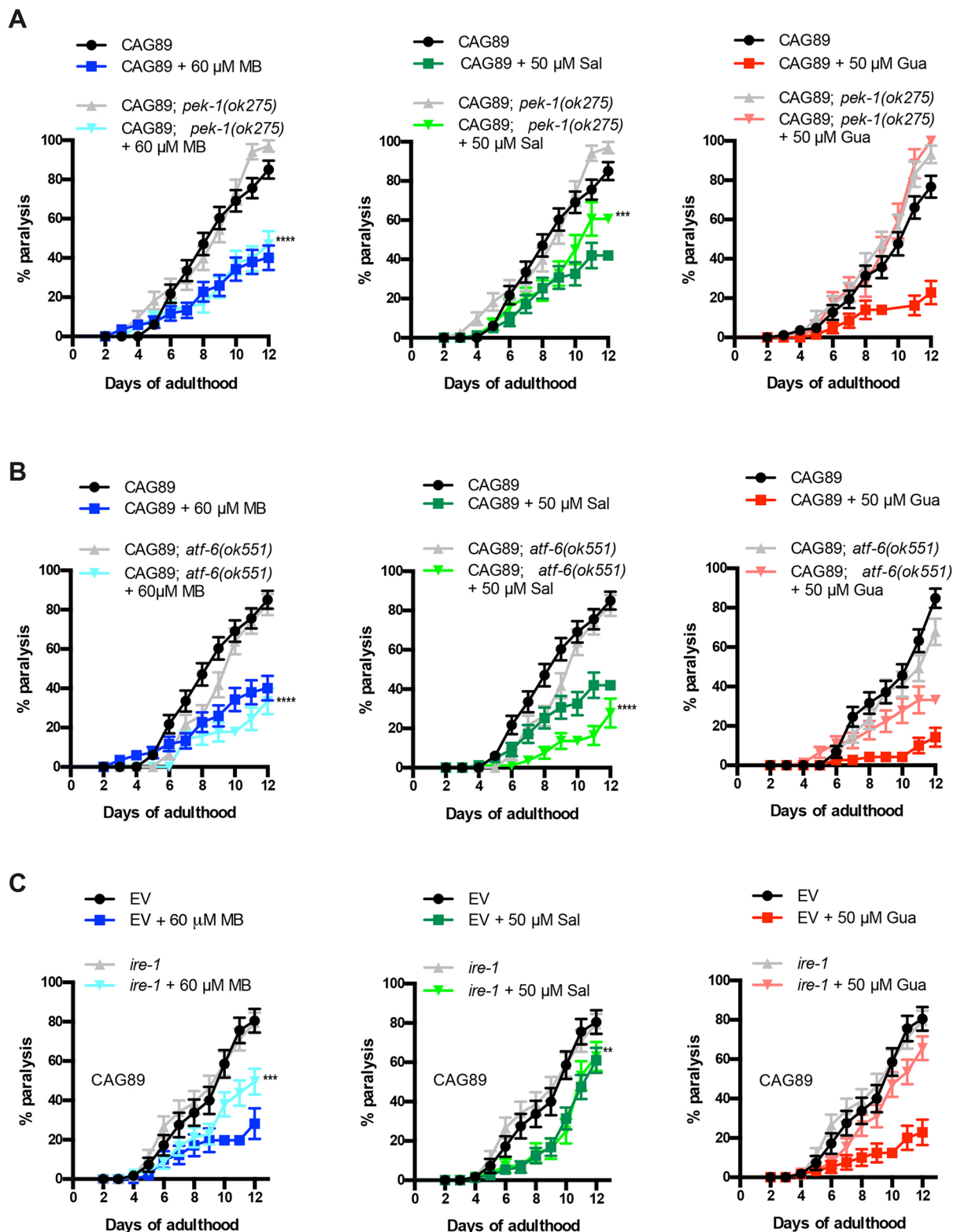


Fig. 8. See next page for legend.

The RNAi clone was obtained from the ORFeome RNAi library (Open Biosystems) and sequence verified. For *ero-1* experiments, age-synchronized worms at adult day 2 were incubated on a slide with 5 μ M 2',7'-dichlorofluorescein diacetate (DCF-DA; Sigma-Aldrich) for 30 min at room temperature and washed three times for 5-10 min with PBS 1 \times (10 mM Na₂HPO₄, 1.8 mM NaH₂PO₄ and 140 mM NaCl, adjusted to pH to

7.4; adding ddH₂O to 1000 ml). Worms were visualized by fluorescence microscopy under 488 nm wavelength excitation.

For *ire-1* experiments, worms were scored from adult day 1 to adult day 12 for paralysis assays. They were transferred to fresh plates every 2 days until the cessation of progeny production. Each condition was done in triplicates with 30-40 worms per plate. All experiments were conducted at 20°C.

Fig. 8. Chemical-genetic approach analysis of UPR^{ER} pathways in ATXN3-CAG89 mutants. (A) Paralysis assays for ATXN3-CAG89 and ATXN3-CAG89; *pek-1(ok275)* transgenic mutant worms in presence of 60 μ M MB, 50 μ M Sal and 50 μ M Gua. We observed that Gua failed to suppress the paralysis in ATXN3-CAG89; *pek-1(ok275)* worms, Sal partly suppressed paralysis ($***P<0.001$) and MB suppressed paralysis in ATXN3-CAG89; *pek-1(ok275)* mutant worms ($****P<0.0001$) [by log-rank (Mantel–Cox) test; $n=270$ –300]. This experiment was repeated three times. (B) ATXN3-CAG89 and ATXN3-CAG89; *atf-6(ok551)* mutant worms were treated with 60 μ M MB, 50 μ M Sal and 50 μ M Gua. We observed that Sal and MB suppressed paralysis in ATXN3-CAG89; *atf-6(ok551)* mutant worms ($****P<0.0001$ for both compounds), contrary to Gua, which is dependent on the *atf-6* branch of the UPR^{ER} pathway, showing an incapacity to suppress the paralysis in the transgenic mutant worms [by log-rank (Mantel–Cox) test; $n=270$ –300]. This experiment was repeated three times. (C) Paralysis assays for *ire-1* RNAi ATXN3-CAG89 worms treated with 60 μ M MB, 50 μ M Sal and 50 μ M Gua. We observed that Gua totally and MB partly ($***P<0.001$) failed to suppress the paralysis in *ire-1* RNAi worms, contrary to Sal, which suppressed paralysis in *ire-1* RNAi worms ($**P<0.01$) [by log-rank (Mantel–Cox) test; $n=270$ –300]. This experiment was repeated three times. Gua, guanabenz; MB, Methylene Blue; Sal, salubrinal; UPR^{ER}, ER unfolded protein response.

Fluorescence microscopy (neurodegeneration, ER stress response and oxidative stress assays)

For scoring of neuronal processes for gaps or breakages, *unc-47::mCherry*; ATXN3-CAG89, *unc-47::mCherry*; ATXN3-CAG10 and *unc-47::mCherry* were collected at adult day 5 for visualization of motoneuron processes *in vivo*. For visualization of the ER stress response, *hsp-4::GFP*, *hsp-4::GFP*; ATXN3-CAG10 and *hsp-4::GFP*; ATXN3-CAG89 worms were collected at adult day 1, and for DCF-DA experiments, wild-type N2 worms and ATXN3 transgenic lines were collected at adult day 2. The nematodes were immobilized using M9 buffer with 60% glycerol and mounted on slides with 2% agarose pads. mCherry was visualized at 595 nm, and GFP was visualized at 488 nm using a Zeiss Axio Imager M2 microscope. Fluorescent expression was visualized with a DIC microscope Zeiss AxioObserver A1. The software used was AxioVs40 4.8.2.0. One hundred worms were scored per condition for the neurodegeneration assays. Approximately 25 worms were visualized per condition for the ER stress response and the oxidative stress experiments. Image processing and quantification were done with Adobe Photoshop. To compare fluorescence in ER stress response and oxidative stress assays, we calculated the changes in the ratio (size/intensity of fluorescence). Student's unpaired *t*-test was used for statistical analysis.

Compound testing on solid media

Worms were exposed from hatching (by synchronization) to 60 μ M Methylene Blue, 50 μ M salubrinal or 50 μ M guanabenz incorporated into NGM solid medium, or to NGM solid medium only as a control. All the plates were streaked with OP50 *E. coli*. Compounds were purchased from Sigma-Aldrich (St Louis, MO, USA) and Tocris Bioscience (Ellisville, MO, USA). Briefly, 30–40 worms were picked and plated on the corresponding NGM medium (30–40 worms per plate for each condition, and each condition was done in triplicates) in order to complete the paralysis and lifespan assays, the neurodegeneration observations (fluorescence microscopy) and the drug screens.

Compound testing in liquid culture

The swimming activity of the nematodes was measured by a WMicroTracker machine (Phylum Tech) (Simonetta and Golombek, 2007). Briefly, worms were exposed until day 5 of adulthood on the corresponding NGM medium plates (drug exposure on solid media) and then were transferred into a 96-well plate. Each well contained a final volume of 100 μ l of the drug with the appropriate concentration or M9 buffer used as control, and ~30 worms adult day 5 (obtained via synchronization). Each condition was done in triplicates, and the experiments were repeated at least three times. The swimming movements of the nematodes were tracked for 10 h.

Reactive oxygen species measurements

The *in vivo* detection of reactive oxygen species in *C. elegans* has been described previously (Vaccaro et al., 2013, 2012a). Briefly, age-

synchronized worms at adult day 2 were incubated on a slide with 5 μ M DCF-DA (Sigma-Aldrich) for 30 min at room temperature and washed three times for 5–10 min with PBS 1 \times (10 mM Na₂HPO₄, 1.8 mM NaH₂PO₄ and 140 mM NaCl, with pH adjusted to 7.4; adding ddH₂O to 1000 ml). Worms were visualized by fluorescence microscopy under a 488 nm wavelength excitation.

Immunofluorescence (antibody staining for transgenic worms)

Five plates of worms for each strain were collected with M9, centrifuged at 3,250 *g* (A-4-81 Rotor) for 4 min at 4°C and washed twice with M9 buffer with the same centrifugation conditions. Worm pellets were placed at –80°C overnight. The supernatants were discarded, and 500 μ l of cold methanol (stored at –20°C for 5 min) was added to the pellets and remained for 5 min at room temperature (fixation step). The supernatants were discarded, and the pellets were washed twice with PBS 1 \times (10 mM Na₂HPO₄, 1.8 mM NaH₂PO₄ and 140 mM NaCl, with pH adjusted to 7.4; adding ddH₂O to 1000 ml) and centrifuged at 2,151 *g* (FA-45-30-11 Rotor) for 3 min at 23°C. The pellets were then blocked with 300 μ l donkey serum solution [0.05 mg/l BSA, 5% donkey serum (Sigma-Aldrich; cat. #: D9663; 10 ml), 0.2% Triton] for 30 min at room temperature. Worms were centrifuged at 2,151 *g* (FA-45-30-11 Rotor) for 3 min at 23°C and the supernatants discarded. Four hundred microlitres of the primary antibody rabbit anti-ATXN3 (1:200; Proteintech; cat. #: 13505-1) in the donkey serum solution was added to the pellets and stored at 4°C overnight. Worms were washed twice with PBS 1 \times for 5 min and each time centrifuged at 2,151 *g* (FA-45-30-11; Rotor) for 1 min at 23°C to discard the supernatants. The supernatants were discarded, and 400 μ l of the secondary antibody donkey anti-rabbit IgG (H+L) Alexa Fluor 488 (1:250; Invitrogen; cat. #: A-21206) in PBS 1 \times was added to the pellets and remained for 30 min at room temperature. Worms were washed with PBS 1 \times , centrifuged at 2,151 *g* (FA-45-30-11 Rotor) for 1 min at room temperature and the supernatants discarded. Pellets were washed with 400 μ l of TOPRO-3 Iodide dye (1:300; Invitrogen; cat. #: T3605) in PBS 1 \times for 5 min, centrifuged at 2,151 *g* (FA-45-30-11 Rotor) for 1 min at 23°C, then washed twice with PBS-T 1 \times (add 1 ml of Tween to PBS 1 \times stock) for 5 min at room temperature. Worms were mounted on slides with 20 μ l mounting solution (Invitrogen ProLong Antifade Kit; cat. #: P7481) and stored at 4°C overnight. Confocal images were acquired on a Leica TCS-SP5 inverted confocal microscope using an HCX PL APO CS 40 \times /1.25 oil objective. Excitation system was performed using a 633 HeNe laser for TOPRO simultaneously with the 488 nm line of an argon laser for eGFP. Scan speed was 400 Hz. Detection bandwidth was 643–800 nm for TOPRO-3, and 498–551 nm for eGFP. The software used was LAS Image Analysis. Twenty-five to thirty worms were visualized per condition for the aggregation phenotype. Image processing was done with LAS Image Analysis and Adobe Photoshop.

Cell lysis

Cells derived from healthy and MJD patients were obtained from Dr Guy Rouleau (Montreal Neurological Institute and Hospital, McGill University). MJD lymphoblastoid cell lines (LCL) were established from peripheral blood samples of MJD patients of European origin. Cells were grown in IMDM (Gibco) supplemented with fetal bovine serum (10%), penicillin and streptomycin (100 units/ml) and L-glutamine (0.292 mg/ml). Collected cells were centrifuged at 98 *g* (FA-45-24-11 Rotor) for 2 min at 4°C. The supernatants were discarded and the pellets transferred into new Eppendorf tubes with 1 ml cold PBS 1 \times (10 mM Na₂HPO₄, 1.8 mM NaH₂PO₄ and 140 mM NaCl, with pH adjusted to 7.4; adding ddH₂O to 1000 ml) and centrifuged at 98 *g* for 5 min at 4°C. This step was repeated three times. The medium was aspirated and the pellets were resuspended in an appropriate volume of RIPA buffer (150 mM NaCl, 50 mM Tris pH 7.4, 1% Triton X-100, 0.1% SDS and 1% sodium deoxycholate) and 0.1% protease inhibitors (10 mg/ml leupeptin, 10 mg/ml pepstatin A and 10 mg/ml chymostatin LPC; 1/1000) depending on pellet size. The samples were put on ice for 10 min, then placed at room temperature for 10 min. The samples were then centrifuged at 142 *g* (FA-45-24-11 Rotor) for 15 min at 4°C. The pellets were discarded, and the supernatants were collected in 1.5 ml tubes and stored at –80°C.

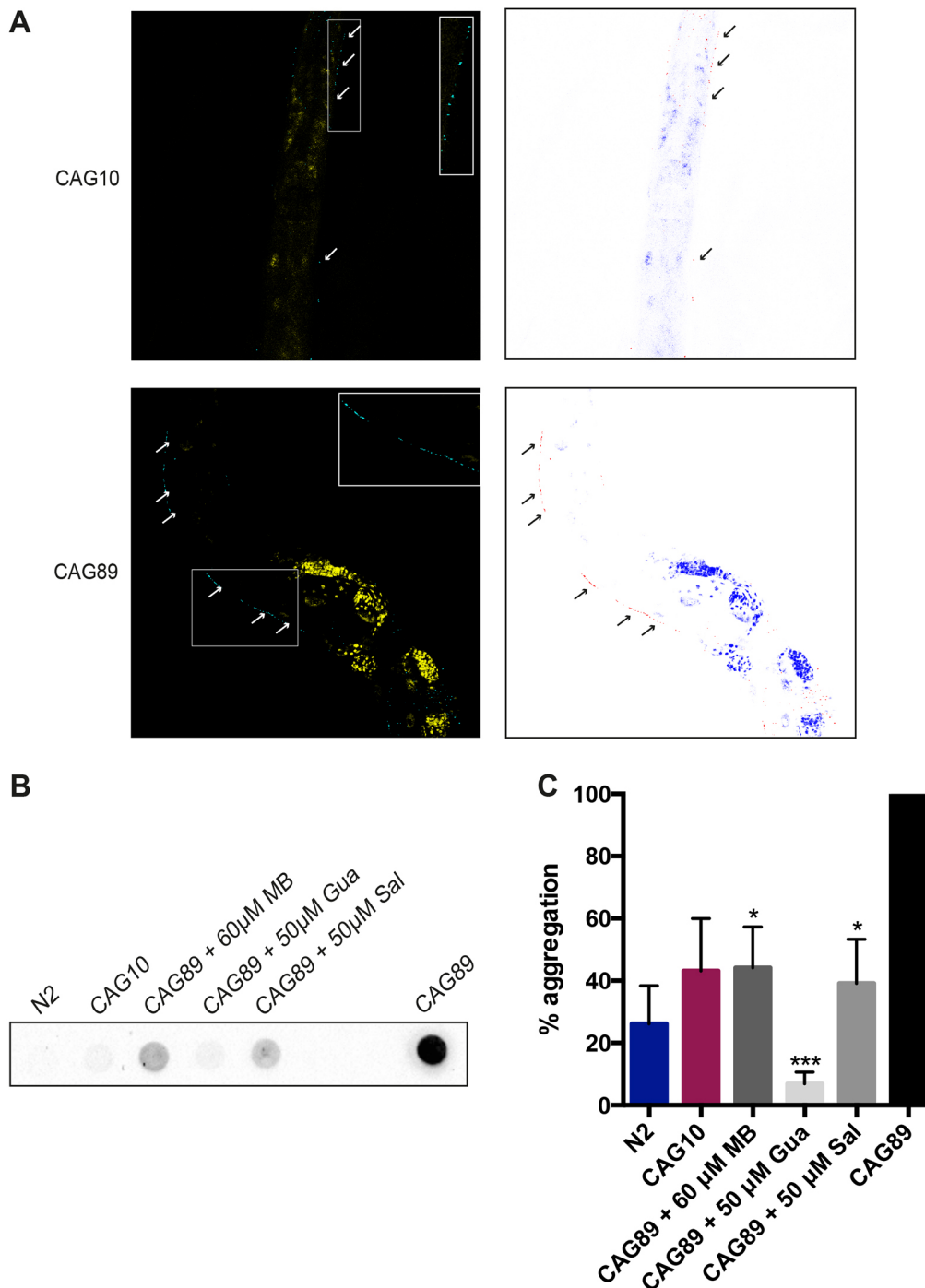


Fig. 9. Small molecule suppression of ATXN3-CAG89 aggregation.

(A) Fixed whole *ATXN3-CAG10* and *ATXN3-CAG89* transgenic worms stained with a human ATXN3 antibody (blue) and TOPRO dye (yellow) for the nucleic acids. Arrows indicate ATXN3 protein in the motoneurons of *ATXN3* transgenics. Second panel is a colour-inverted image to aid visualization. The insets are magnifications of the aggregates indicated in the transgenic worms with a dashed line box. (B) Total protein levels for N2 and transgenic worms expressing *ATXN3-CAG10* or mutant *ATXN3-CAG89*. Antibody detection revealed high accumulation of the *ATXN3-CAG89* in the pelleted, insoluble fraction, when compared with *ATXN3-CAG10* and N2 wild-type worms. There was a reduction of aggregation in *ATXN3-CAG89* worms when treated with 60 μ M MB, 50 μ M Sal or 50 μ M Gua. Gua was especially potent in reducing protein aggregation. (C) Quantification of the intensity of the aggregation in transgenic *ATXN3-CAG89* mutants and wild-type N2 and *ATXN3-CAG10* worms. There was a significant increase of aggregation in *ATXN3-CAG89* when compared with the wild-type N2 and *ATXN3-CAG10* worms. After treatment with 60 μ M MB (* P <0.05), 50 μ M Sal (* P <0.05) or 50 μ M Gua (** P <0.001) (by ANOVA) *ATXN3-CAG89* showed a significant decrease in aggregation levels. Gua, guanabenz; MB, Methylene Blue; Sal, salubrinol.

Western blotting

Fifteen plates of worms for each strain and for each condition (with or without compounds) were collected with M9, centrifuged at 3,250 g (A-4-81 Rotor) for 4 min at 4°C and washed twice with M9 buffer with the same centrifugation conditions. Worm pellets were placed at -80°C overnight. Pellets were lysed in RIPA buffer (150 mM NaCl, 50 mM Tris pH 7.4, 1% Triton X-100, 0.1% SDS and 1% sodium deoxycholate) and 0.1% protease inhibitors (10 mg/ml leupeptin, 10 mg/ml pepstatin A and 10 mg/ml chymostatin LPC; 1/1000). Pellets were passed through a 27.5-gauge syringe seven times, sonicated for 5 min, and centrifuged at 16,000 g for 15 min at 4°C. Supernatants were collected in 1.5 ml tubes. The supernatants were quantified using the BCA protein assay kit (Thermo Scientific) following the manufacturer's protocol and instructions.

Thirty-five micrograms per well of protein were loaded in a 10% polyacrylamide gel for 80 min, transferred to nitrocellulose membranes (BioRad) and immunoblotted. Antibodies used were as follows: rabbit anti-ATXN3 (1:500; Proteintech; cat. #: 13505-1) and mouse anti-Actin (1:2500; MP Biomedical; cat. #: 691001). Blots were visualized using peroxidase-conjugated secondary antibodies and ECL western blotting substrate (Thermo Scientific). N2 wild-type worms and *atx-3(tm1689)* were used as controls. The ladder used was Precision Plus Protein Kaleidoscope (BioRad). Densitometry was performed with Adobe Photoshop.

Protein solubility

Fifteen plates of worms for each strain and for each condition (*ATXN3-CAG89* worms treated with each compound) were collected with M9, centrifuged at 3,250 g (A-4-81 Rotor) for 4 min at 4°C and washed twice

with M9 buffer with the same centrifugation conditions. Worm pellets were placed at -80°C overnight. To obtain soluble and insoluble fractions for our transgenics, worms were lysed in extraction buffer (1 M Tris-HCl pH 8, 0.5 M EDTA, 1 M NaCl and 10% SDS) plus protease inhibitors (10 mg/ml leupeptin, 10 mg/ml pepstatin A and 10 mg/ml chymostatin LPC; 1/1000). Pellets were passed through a 27.5-gauge syringe 10 times, sonicated for 5 min, and centrifuged at 16,000 *g* for 15 min at 4°C . The soluble supernatants were collected in 1.5 ml tubes and stored at -80°C . The remaining pellets were resuspended in extraction buffer, sonicated and centrifuged at 10,000 *g* for 5 min. The supernatants were discarded and the remaining pellets resuspended in 100 μl of RIPA buffer and sonicated for ~ 90 min until the pellets were resuspended in solution. The pellets were collected and stored in 1.5 ml tubes at -80°C . The supernatants and pellets were quantified using the BCA protein assay kit (Thermo Scientific) following the manufacturer's protocol and instructions.

Dot blotting

Dot blotting was done using the Bio-Dot SF microfiltration apparatus (cat. #: 170-6542). The assays were done using the manufacturer's protocol and instructions following the section Protein Slot Blotting-Immunoassays procedure and followed immunoblotting procedures. The antibody used was rabbit anti-ATXN3 (1:500; Proteintech; cat. #: 13505-1). Blots were visualized using peroxidase-conjugated secondary antibodies and ECL western blotting substrate (Thermo Scientific) via the Bio Rad ChemiDoc MP Imaging System (model #: Universal HOOD III). N2 wild-type worms and *ATXN3-CAG10* were used as controls. Quantification was performed with Image Lab software.

Statistics

Paralysis and lifespan curves were generated and compared using the log-rank (Mantel-Cox) test. All experiments were repeated at least three times. For neurodegeneration, the drug screening and the fluorescence tests (oxidative stress and ER stress response), Student's unpaired *t*-tests were performed. For the dot blotting quantification, ANOVAs were used. Prism 6 (GraphPad Software) was used for all statistical analyses.

Acknowledgements

Some worm strains were provided by the Caenorhabditis Genetics Center which is funded by NIH Office of Research Infrastructure Programs (P40 OD010440). Special thanks to Dr Guy Rouleau (Montreal Neurological Institute and Hospital, McGill University) for providing human cDNAs ATXN3 and cell lines for healthy and MJD patients, Dr Erik Jorgensen (University of Utah) for providing clones containing the *unc-47* promoter, and Dr Geraldine Seydoux (Johns Hopkins; Addgene plasmid 17253) for the *unc-54* 3'UTR plasmid pCM5.37. Special thanks to the cell imaging core facility of CRCHUM for confocal microscopy. Special thanks to Alexandre Desjardins (research assistant) in Dr Nicole Leclerc's laboratory for his help concerning the dot blotting assays. A very special thanks to a few members of our laboratory for their presence, help and technical assistance: C. Bretonneau, S. Oré Rodriguez, J. Vérièpe and S. Peyrard.

Competing interests

The authors declare no competing or financial interests.

Author contributions

Conceptualization: J.A.P.; Methodology: Y.F., A.T., S.G., J.A.P.; Validation: Y.F.; Formal analysis: Y.F.; Investigation: Y.F.; Resources: Y.F.; Writing - original draft: Y.F., J.A.P.; Writing - review & editing: Y.F., J.A.P.; Visualization: Y.F., J.A.P.; Supervision: J.A.P.; Project administration: Y.F.; Funding acquisition: J.A.P.

Funding

This work was supported by the Canadian Institutes of Health Research (to J.A.P.).

Supplementary information

Supplementary information available online at <http://dmm.biologists.org/lookup/doi/10.1242/dmm.029736.supplemental>

References

Bettencourt, C., Santos, C., Kay, T., Vasconcelos, J. and Lima, M. (2008). Analysis of segregation patterns in Machado-Joseph disease pedigrees. *J. Hum. Genet.* **53**, 920-923.

Bonanomi, M., Natalello, A., Visentin, C., Pastori, V., Penco, A., Cornelli, G., Colombo, G., Malabarba, M. G., Doglia, S. M., Relini, A. et al. (2014). Epigallocatechin-3-gallate and tetracycline differently affect ataxin-3 fibrillogenesis and reduce toxicity in spinocerebellar ataxia type 3 model. *Hum. Mol. Genet.* **23**, 6542-6552.

Breuer, P., Haacke, A., Evert, B. O. and Wüllner, U. (2010). Nuclear aggregation of polyglutamine-expanded ataxin-3: fragments escape the cytoplasmic quality control. *J. Biol. Chem.* **285**, 6532-6537.

C. elegans Deletion Mutant Consortium. (2012). large-scale screening for targeted knockouts in the *Caenorhabditis elegans* genome. *G3 (Bethesda)*. **2**, 1415-1425.

Catoire, H., Pasco, M. Y., Abu-Baker, A., Holbert, S., Tourette, C., Brais, B., Rouleau, G. A., Parker, J. A. and Néri, C. (2008). Sirtuin inhibition protects from the polyalanine muscular dystrophy protein PABPN1. *Hum. Mol. Genet.* **17**, 2108-2117.

Christie, N. T. M., Lee, A. L., Fay, H. G., Gray, A. A. and Kikis, E. A. (2014). Novel polyglutamine model uncouples proteotoxicity from aging. *PLoS ONE* **9**, e96835.

Collins, J. J., Huang, C., Hughes, S. and Kornfeld, K. (2008). The measurement and analysis of age-related changes in *Caenorhabditis elegans*. *WormBook*, 1-21.

Costa, M. C. and Paulson, H. L. (2012). Toward understanding Machado-Joseph disease. *Prog. Neurobiol.* **97**, 239-257.

Cummings, C. J. and Zoghbi, H. Y. (2000). Fourteen and counting: unraveling trinucleotide repeat diseases. *Hum. Mol. Genet.* **9**, 909-916.

Echtemeyer, C., da Fontoura Costa, L., Rodrigues, F. A. and Kaiser, M. (2011). Automatic network fingerprinting through single-node motifs. *PLoS ONE* **6**, e15765.

Evers, M. M., Toonen, L. J. and van Roon-Mom, W. M. (2014). Ataxin-3 protein and RNA toxicity in spinocerebellar ataxia type 3: current insights and emerging therapeutic strategies. *Mol. Neurobiol.* **49**, 1513-1531.

França, M. C., Jr, D'Abreu, A., Nucci, A. and Lopes-Cendes, I. (2008). Muscle excitability abnormalities in Machado-Joseph disease. *Arch. Neurol.* **65**, 525-529.

Frokjaer-Jensen, C., Davis, M. W., Sarov, M., Taylor, J., Filibotte, S., LaBella, M., Pozniakovskiy, A., Moerman, D. G. and Jorgensen, E. M. (2014). Random and targeted transgene insertion in *Caenorhabditis elegans* using a modified Mos1 transposon. *Nat. Methods* **11**, 529-534.

Gatchel, J. R. and Zoghbi, H. Y. (2005). Diseases of unstable repeat expansion: mechanisms and common principles. *Nat. Rev. Genet.* **6**, 743-755.

Goto, J., Watanabe, M., Ichikawa, Y., Yee, S.-B., Ihara, N., Endo, K., Igarashi, S., Takiyama, Y., Gaspar, C., Maciel, P. et al. (1997). Machado-Joseph disease gene products carrying different carboxyl termini. *Neurosci. Res.* **28**, 373-377.

Harding, H. P., Zhang, Y., Zeng, H., Novoa, I., Lu, P. D., Calfon, M., Sadri, N., Yun, C., Popko, B., Paules, R. et al. (2003). An integrated stress response regulates amino acid metabolism and resistance to oxidative stress. *Mol. Cell* **11**, 619-633.

Herndon, L. A., Schmeissner, P. J., Dudaronek, J. M., Brown, P. A., Listner, K. M., Sakano, Y., Paupard, M. C., Hall, D. H. and Driscoll, M. (2002). Stochastic and genetic factors influence tissue-specific decline in ageing *C. elegans*. *Nature* **419**, 808-814.

Julien, C., Lissouba, A., Madabattula, S., Fardghassemi, Y., Rosenfelt, C., Androschuk, A., Strautman, J., Wong, C., Bysice, A., O'Sullivan, J. et al. (2016). Conserved pharmacological rescue of hereditary spastic paraplegia-related phenotypes across model organisms. *Hum. Mol. Genet.* **25**, 1088-1099.

Kanai, K. and Kuwabara, S. (2009). Motor nerve hyperexcitability and muscle cramps in Machado-Joseph disease. *Arch. Neurol.* **66**, 139; author reply 139-140.

Kawaguchi, Y., Okamoto, T., Taniwaki, M., Aizawa, M., Inoue, M., Katayama, S., Kawakami, H., Nakamura, S., Nishimura, M., Akiguchi, I. et al. (1994). CAG expansions in a novel gene for Machado-Joseph disease at chromosome 14q32.1. *Nat. Genet.* **8**, 221-228.

Khan, L. A., Bauer, P. O., Miyazaki, H., Lindenberg, K. S., Landwehrmeyer, B. G. and Nukina, N. (2006). Expanded polyglutamines impair synaptic transmission and ubiquitin-proteasome system in *Caenorhabditis elegans*. *J. Neurochem.* **98**, 576-587.

Koch, P., Breuer, P., Peitz, M., Jungverdorben, J., Kesavan, J., Poppe, D., Doerr, J., Ladewig, J., Mertens, J., Tuting, T. et al. (2011). Excitation-induced ataxin-3 aggregation in neurons from patients with Machado-Joseph disease. *Nature* **480**, 543-546.

Li, X., Liu, H., Fischhaber, P. L. and Tang, T.-S. (2015). Toward therapeutic targets for SCA3: insight into the role of Machado-Joseph disease protein ataxin-3 in misfolded proteins clearance. *Prog. Neurobiol.* **132**, 34-58.

Loria, P. M., Hodgkin, J. and Hobert, O. (2004). A conserved postsynaptic transmembrane protein affecting neuromuscular signaling in *Caenorhabditis elegans*. *J. Neurosci.* **24**, 2191-2201.

Maciel, P., Costa, M. C., Ferro, A., Rousseau, M., Santos, C. S., Gaspar, C., Barros, J., Rouleau, G. A., Coutinho, P. and Sequeiros, J. (2001). Improvement in the molecular diagnosis of Machado-Joseph disease. *Arch. Neurol.* **58**, 1821-1827.

Mahoney, T. R., Luo, S. and Nonet, M. L. (2006). Analysis of synaptic transmission in *Caenorhabditis elegans* using an aldicarb-sensitivity assay. *Nat. Protoc.* **1**, 1772-1777.

- Matos, C. A., de Macedo-Ribeiro, S. and Carvalho, A. L. (2011). Polyglutamine diseases: the special case of ataxin-3 and Machado-Joseph disease. *Prog. Neurobiol.* **95**, 26-48.
- McIntire, S. L., Jorgensen, E., Kaplan, J. and Horvitz, H. R. (1993). The GABAergic nervous system of *Caenorhabditis elegans*. *Nature* **364**, 337-341.
- McIntire, S. L., Reimer, R. J., Schuske, K., Edwards, R. H. and Jorgensen, E. M. (1997). Identification and characterization of the vesicular GABA transporter. *Nature* **389**, 870-876.
- Petrash, H. A., Philbrook, A., Haburcak, M., Barbagallo, B. and Francis, M. M. (2013). ACR-12 ionotropic acetylcholine receptor complexes regulate inhibitory motor neuron activity in *Caenorhabditis elegans*. *J. Neurosci.* **33**, 5524-5532.
- Piano, F., Schetter, A. J., Morton, D. G., Gunsalus, K. C., Reinke, V., Kim, S. K. and Kemphues, K. J. (2002). Gene clustering based on RNAi phenotypes of ovary-enriched genes in *C. elegans*. *Curr. Biol.* **12**, 1959-1964.
- Pinto, S. and De Carvalho, M. (2008). Machado-Joseph disease presenting as motor neuron disease. *Amyotroph. Lateral. Scler.* **9**, 188-191.
- Reina, C. P., Zhong, X. and Pittman, R. N. (2010). Proteotoxic stress increases nuclear localization of ataxin-3. *Hum. Mol. Genet.* **19**, 235-249.
- Riess, O., Rüb, U., Pastore, A., Bauer, P. and Schöls, L. (2008). SCA3: neurological features, pathogenesis and animal models. *Cerebellum* **7**, 125-137.
- Rodrigues, A. J., Coppola, G., Santos, C., Costa Mdo, C., Ailion, M., Sequeiros, J., Geschwind, D. H. and Maciel, P. (2007). Functional genomics and biochemical characterization of the *C. elegans* orthologue of the Machado-Joseph disease protein ataxin-3. *FASEB J.* **21**, 1126-1136.
- Rodrigues, A. J., Neves-Carvalho, A., Teixeira-Castro, A., Rokka, A., Corthals, G., Logarinho, E. and Maciel, P. (2011). Absence of ataxin-3 leads to enhanced stress response in *C. elegans*. *PLoS ONE* **6**, e18512.
- Rub, U., de Vos, R. A. I., Schultz, C., Brunt, E. R., Paulson, H. and Braak, H. (2002). Spinocerebellar ataxia type 3 (Machado-Joseph disease): severe destruction of the lateral reticular nucleus. *Brain* **125**, 2115-2124.
- Rub, U., Brunt, E. R. and Deller, T. (2008). New insights into the pathoanatomy of spinocerebellar ataxia type 3 (Machado-Joseph disease). *Curr. Opin. Neurol.* **21**, 111-116.
- Saxena, S. and Caroni, P. (2011). Selective neuronal vulnerability in neurodegenerative diseases: from stressor thresholds to degeneration. *Neuron* **71**, 35-48.
- Schmeisser, K., Fardghassemi, Y. and Parker, J. A. (2017). A rapid chemical-genetic screen utilizing impaired movement phenotypes in *C. elegans*: Input into genetics of neurodevelopmental disorders. *Exp. Neurol.* **293**, 101-114.
- Schöls, L., Bauer, P., Schmidt, T., Schulte, T. and Riess, O. (2004). Autosomal dominant cerebellar ataxias: clinical features, genetics, and pathogenesis. *Lancet. Neurol.* **3**, 291-304.
- Shao, J. and Diamond, M. I. (2007). Polyglutamine diseases: emerging concepts in pathogenesis and therapy. *Hum. Mol. Genet.* **16**, R115-R123.
- Simonetta, S. H. and Golombek, D. A. (2007). An automated tracking system for *Caenorhabditis elegans* locomotor behavior and circadian studies application. *J. Neurosci. Methods* **161**, 273-280.
- Soon, B.-W., Cheng, C.-H., Liu, R.-S. and Shan, D.-E. (1997). Machado-Joseph disease: clinical, molecular, and metabolic characterization in Chinese kindreds. *Ann. Neurol.* **41**, 446-452.
- Stiernagle, T. (2006). Maintenance of *C. elegans*. *WormBook*, 1-11.
- Stochmanski, S. J., Therrien, M., Laganière, J., Rochefort, D., Laurent, S., Karamera, L., Gaudet, R., Vyboh, K., Van Meyel, D. J., Di Cristo, G. et al. (2012). Expanded ATXN3 frameshifting events are toxic in *Drosophila* and mammalian neuron models. *Hum. Mol. Genet.* **21**, 2211-2218.
- Takiyama, Y., Oyanagi, S., Kawashima, S., Sakamoto, H., Saito, K., Yoshida, M., Tsuji, S., Mizuno, Y. and Nishizawa, M. (1994). A clinical and pathologic study of a large Japanese family with Machado-Joseph disease tightly linked to the DNA markers on chromosome 14q. *Neurology* **44**, 1302-1308.
- Taylor, R. C. and Dillin, A. (2013). XBP-1 is a cell-nonautonomous regulator of stress resistance and longevity. *Cell* **153**, 1435-1447.
- Teixeira-Castro, A., Ailion, M., Jalles, A., Brignull, H. R., Vilaça, J. L., Dias, N., Rodrigues, P., Oliveira, J. F., Neves-Carvalho, A., Morimoto, R. I. et al. (2011). Neuron-specific proteotoxicity of mutant ataxin-3 in *C. elegans*: rescue by the DAF-16 and HSF-1 pathways. *Hum. Mol. Genet.* **20**, 2996-3009.
- Teixeira-Castro, A., Jalles, A., Esteves, S., Kang, S., da Silva Santos, L., Silva-Fernandes, A., Neto, M. F., Briellmann, R. M., Bessa, C., Duarte-Silva, S. et al. (2015). Serotonergic signalling suppresses ataxin 3 aggregation and neurotoxicity in animal models of Machado-Joseph disease. *Brain* **138**, 3221-3237.
- Therrien, M. and Parker, J. A. (2014). Worming forward: amyotrophic lateral sclerosis toxicity mechanisms and genetic interactions in *Caenorhabditis elegans*. *Front. Genet.* **5**, 85.
- Urano, F., Calfon, M., Yoneda, T., Yun, C., Kiraly, M., Clark, S. G. and Ron, D. (2002). A survival pathway for *Caenorhabditis elegans* with a blocked unfolded protein response. *J. Cell Biol.* **158**, 639-646.
- Vaccaro, A., Patten, S. A., Ciura, S., Maiores, C., Therrien, M., Drapeau, P., Kabashi, E. and Parker, J. A. (2012a). Methylene blue protects against TDP-43 and FUS neuronal toxicity in *C. elegans* and *D. rerio*. *PLoS ONE* **7**, e42117.
- Vaccaro, A., Tauffenberger, A., Aggad, D., Rouleau, G., Drapeau, P. and Parker, J. A. (2012b). Mutant TDP-43 and FUS cause age-dependent paralysis and neurodegeneration in *C. elegans*. *PLoS ONE* **7**, e31321.
- Vaccaro, A., Tauffenberger, A., Ash, P. E. A., Carlomagno, Y., Petrucelli, L. and Parker, J. A. (2012c). TDP-1/TDP-43 regulates stress signaling and age-dependent proteotoxicity in *Caenorhabditis elegans*. *PLoS Genet.* **8**, e1002806.
- Vaccaro, A., Patten, S. A., Aggad, D., Julien, C., Maiores, C., Kabashi, E., Drapeau, P. and Parker, J. A. (2013). Pharmacological reduction of ER stress protects against TDP-43 neuronal toxicity in vivo. *Neurobiol. Dis.* **55**, 64-75.
- van de Warrenburg, B. P. C., Sinke, R. J., Verschuuren-Bemelmans, C. C., Scheffer, H., Brunt, E. R., Ippel, P. F., Maat-Kievit, J. A., Dooijes, D., Notermans, N. C., Lindhout, D. et al. (2002). Spinocerebellar ataxias in the Netherlands: prevalence and age at onset variance analysis. *Neurology* **58**, 702-708.
- van Oosten-Hawle, P., Porter, R. S. and Morimoto, R. I. (2013). Regulation of organismal proteostasis by transcellular chaperone signaling. *Cell* **153**, 1366-1378.
- Veriepe, J., Fossouo, L. and Parker, J. A. (2015). Neurodegeneration in *C. elegans* models of ALS requires TIR-1/Sarm1 immune pathway activation in neurons. *Nat. Commun.* **6**, 7319.
- Walker, A. K. and Atkin, J. D. (2011). Stress signaling from the endoplasmic reticulum: a central player in the pathogenesis of amyotrophic lateral sclerosis. *IUBMB Life* **63**, 754-763.
- Wang, J., Farr, G. W., Hall, D. H., Li, F., Furtak, K., Dreier, L. and Horwich, A. L. (2009). An ALS-linked mutant SOD1 produces a locomotor defect associated with aggregation and synaptic dysfunction when expressed in neurons of *Caenorhabditis elegans*. *PLoS Genet.* **5**, e1000350.
- Wüllner, U., Reimold, M., Abele, M., Bürk, K., Minnerop, M., Dohmen, B.-M., Machulla, H.-J., Bares, R. and Klockgether, T. (2005). Dopamine transporter positron emission tomography in spinocerebellar ataxias type 1, 2, 3, and 6. *Arch. Neurol.* **62**, 1280-1285.
- Xu, Z., Joel Tito, A., Rui, Y.-N. and Zhang, S. (2015). Studying polyglutamine diseases in *Drosophila*. *Exp. Neurol.* **274**, 25-41.
- Yen, T. C., Lu, C. S., Tzen, K. Y., Wey, S. P., Chou, Y. H., Weng, Y. H., Kao, P. F. and Ting, G. (2000). Decreased dopamine transporter binding in Machado-Joseph disease. *J. Nucl. Med.* **41**, 994-998.